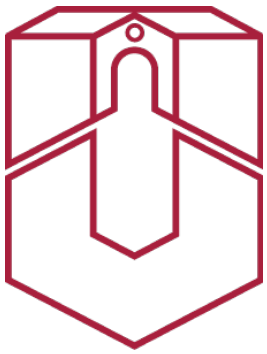

University Osnabrück
Faculty of Physics

Influence of interactions on the efficiency at maximal power of a microscopic thermodynamic machine

Lukas Helmig
October 15, 2021

BACHELOR THESIS

First examiner: **Prof. Dr. P. Maaß**
Second examiner: **D. Lips, M. Sc.**

Abstract

Statistical Physics Research group
Faculty of Physics, University Osnabrück

Influence of interactions on the efficiency at maximal power of a microscopic thermodynamic machine

by Lukas Helmig

A thesis presented for the degree of
Bachelor of Science (B. Sc.)

In dieser Bachelorarbeit wird ein Minimalmodell, was durch eine Mastergleichung beschrieben wird, untersucht. Im Gegensatz zu schon untersuchten Systemen bezieht das Minimalmodell Wechselwirkung zwischen Teilchen ein. Daraus resultiert, dass die "strong coupling" Eigenschaft verloren geht. Das Minimalmodell wird teils analytisch und teils numerisch bezüglich der Leistung optimiert. Sowohl die Abhängigkeit der Leistung als auch der Systemparameter von der Wechselwirkungsenergie werden am Punkt der maximalen Leistung untersucht. Die Effizienz am Punkt der maximalen Leistung wird in Carnot-Effizienz entwickelt. Der lineare Koeffizient dieser Entwicklung zeigt eine Abhängigkeit von der Wechselwirkungsenergie. Weiter wird eine bewiesene obere Grenze für diesen linearen Koeffizienten für positive Wechselwirkungsenergien gebrochen. Da die obere Grenze mithilfe der linearen irreversiblen Thermodynamik bewiesen wurde, wirft das Ergebis Fragen über Unstimmigkeiten zwischen der stochastischen Thermodynamik und der linearen irreversiblen Thermodynamik auf.

A minimal model governed by a master equation is investigated. In contrast to earlier studied systems, the minimal model includes particle interaction. A result of the integrated interaction is that the strong coupling property is broken. The minimal model is optimized with regard to maximum power using an analytical approach and numerics. The influence of the interaction energy on system parameters, power output, and efficiency at maximum power is illustrated. The linear coefficient of an expansion of the efficiency at maximum power shows a dependence on the interaction energy. A supposed upper bound for the linear coefficient is overcome for positive interaction energies. This leads to concerns about inconsistencies between stochastic thermodynamics and linear irreversible thermodynamics.

I would give everything I know,
for half of what I do not know.

RENÉ DESCARTES

Declaration of originality

Erklärung zur selbstständigen Abfassung der Bachelorarbeit

Name: **Lukas Helmig**

Geburtsdatum: **14.07.1999**

Matrikelnummer: **979556**

Titel der Bachelorarbeit: **Influence of interactions on the efficiency at maximal power of a microscopic thermodynamic machine [Einfluss von Wechselwirkungen auf die Effizienz bei maximaler Leistung einer mikroskopischen thermodynamischen Maschine]**

Ich versichere, dass ich die eingereichte Bachelorarbeit selbstständig und ohne unerlaubte Hilfe verfasst habe. Anderer als der von mir angegebenen Hilfsmittel und Schriften habe ich mich nicht bedient. Alle wörtlich oder sinngemäß den Schriften anderer Autoren entnommenen Stellen habe ich kenntlich gemacht.

I declare that I have written the submitted Bachelor thesis independently and without unauthorised assistance. I have not made use of any aids or writings other than those indicated by me. I have marked all passages taken verbatim or in spirit from the writings of other authors.

Ort, Datum

Unterschrift

Acknowledgement

First, I want to thank Prof. Philipp Maaß for the opportunity to work on such an exciting topic. His guidance and feedback really helped me a lot throughout the entire thesis. I also thank Dominik Lips for the fruitful discussions and for all the time he spent explaining things to me.

Thank you to all the members of the research group who gave me a warm welcome and always had time to listen. It felt nice to be part of the group. I could not imagine a better atmosphere to do research and to work on a thesis. And I do not want to miss having shared an office with Knut, Björn and Johannes. This led to endless discussions, which were not always related to the subject.

Also, I express my gratitude to the Wilhelm-Karmann-Stiftung which supported me financially for the majority of my degree.

Last, I want to thank my family and my girlfriend Jessica who supported me during the hard times of the thesis and kept my motivation high. I thank all my friends who proofread and made suggestions for improvements.

Contents

1. Introduction

When humans started to construct thermodynamic machines, specifically heat engines, the starting point for industrialization was set, which ultimately led us to the modern age. Thermodynamics as a science was born out of the desire to improve the efficiency and power output of heat engines. One of the early major scientific publications was from Sadi Carnot, who wrote about heat, power and efficiency [4]. Back then, the book was so disruptive and innovative that the Carnot engine and the Carnot efficiency are named after Sadi Carnot. This publication was the starting point for modern thermodynamics and led to the formulation of the second law by Clausius [5] and Kelvin [23].
Today, the desire to maximize the power output and the efficiency of a thermodynamic machine is as strong as in those days. The only difference is that we are not talking about large heat engines and combustion engines, but about microscopic thermodynamic systems. Because the experimental methods have improved significantly over the years, microscopic thermodynamic engines can be observed and experimentally investigated, e.g. biological molecular machines and quantum dots [3, 14]. From the theoretical side, microscopic engines have been investigated earlier. These microscopic engines operate in so-called steady states, which are non-equilibrium states. For the description of the nanoscale machines, microscopic non-equilibrium thermodynamics is needed. The foundation of macroscopic non-equilibrium thermodynamics was laid by Lars Onsager with a proof of the reciprocal relations [15]. To describe microscopic non-equilibrium thermodynamics and steady states, stochastic thermodynamics was developed [25]. With this framework, the maximum power and the efficiency at maximum power of microscopic machines could be studied. A lot of different microscopic systems have been subject to investigation, ranging from a simple quantum dot to maser models and Brownian heat engines [8, 1, 12, 18, 20]. The focus laid heavily on the efficiency at maximum power because for microscopic engines with a specific property (so-called strong coupling), old results from macroscopic thermodynamics were reproduced [8, 18, 11]. In 1975, Curzon and Ahlborn optimized a Carnot engine with the condition of irreversible heat flow from reservoirs and obtained an expression of the efficiency at maximum power [7]. The derived efficiency has been called Curzon-Ahlborn efficiency and proved to accurately describe the efficiency of power plants. And surprisingly, microscopic systems with strong coupling agree with this macroscopic result at least to linear order. First, some results raised questions about the universality of the linear coefficient. Later, it was proved that the linear coefficient is indeed universal for strong coupling and universality can be extended to the quadratic

order for a specific symmetry [9]. For microscopic systems in the linear response regime, it has been shown that an upper bound for the linear coefficient exists [24]. To conclude, a lot of effort and time has been put into the investigation of microscopic systems with the strong coupling property. But strong coupling is an idealization because it neglects particle interaction. The goal of this work is to investigate the maximum power and the efficiency of maximum power of a system incorporating particle interaction and breaking strong coupling. In the future, the field of microscopic machines can be backed by data from more accurate experimental methods. So, this work is not entirely of theoretical interest. In Sec. 2, basic concepts of thermodynamics are recapped. Also, the Curzon-Ahlborn efficiency is derived, because it is rarely addressed in undergraduate lectures. In Sec. 3, the principle of microscopic reversibility, thermodynamic forces and Onsager coefficients will be presented to provide an introduction to linear irreversible thermodynamics. As a definition of stochastic thermodynamics can be built on the foundations of the master equation, the master equation will be derived and introduced in Sec. 4. As explained, stochastic thermodynamics is then built up with the master equation in Sec. 5. Finally, the minimal model can be investigated regarding maximum power, see Sec. 6.

2. An introduction to thermodynamics

Thermodynamic systems can be classified as *isloated*, *closed* and *open* depending on how the system is in contact with its environment. Isolated systems can not exchange heat or particles and closed systems are only able to exchange heat. In contrast, open systems can transfer heat and particles. A state function $f(Z_1, \ldots, Z_n)$ can be associated with a thermodynamic system, which describes the behavior of the system with regards to the thermodynamic state variables Z_1 to Z_n. The state variables are either *intensive* or *extensive*. Generally speaking, the state variables are dependent on time. However, most systems reach an equilibrium state after a certain amount of time, where the state variables stay constant. This observation can be used to define a naive concept of an equilibrium state, which is not at all sufficient. A system can be in a non-equilibrium state while the state variables reach a constant level. The studied model in this work is part of non-equilibrium thermodynamics and gives a perfect counterexample for this definition.

2.1. First law

The first law of thermodynamics is an energy conservation law. A change of internal energy ΔE has to be the result of a heat flow $\Delta_{\mathcal{C}} Q$ into the system or an amount of work $\Delta_{\mathcal{C}} W$ that is done on the system. The notation $\Delta_{\mathcal{C}}$ was chosen to highlight the fact that the contribution of heat and work is depending on a specific path $\mathcal{C}$ in the space of state variables. If heat is absorbed by the system, the sign is positive.

$$\Delta E = \Delta_{\mathcal{C}} Q + \Delta_{\mathcal{C}} W \tag{2.1a}$$

$$\mathrm{d}E = đQ + đW. \tag{2.1b}$$

In Eq. (2.1b), a microscopic change of the internal energy is expressed in form of a differential. The left side of the equation is in fact a total differential. As the internal energy is a state function, the change of internal energy is independent of the path in the space of state variables. In contrast, the change of heat and work is mathematically a one-form differential but not a total differential. The independence of the path in the space of state variables is not given. Hence, the change of heat and work is denoted with đ. The formulation of the second law by Clausius [5] led to the introduction of the entropy as a state function.

The entropy S is given by

$$S(z) = S(z_0) + \int_{\mathcal{C}(z_0 \to z)} \frac{đQ_{rev}}{T} \tag{2.2a}$$

$$\mathrm{d}S = \frac{đQ_{rev}}{T}, \tag{2.2b}$$

where z_0 is a start point in the state space of thermodynamic variables, z an end point in state space and $đQ_{\mathrm{rev}}$ is the change of heat during a reversible process. The inverse temperature is therefore an integrating factor for the one-form differential $đQ_{\mathrm{rev}}$. In Eq. (2.2b), the entropy is written as a differential. The introduction of entropy leads to Gibb's fundamental law

$$\mathrm{d}E = T\,\mathrm{d}S - p\,\mathrm{d}V + \mu\,\mathrm{d}N. \tag{2.3}$$

Here T is the temperature, p denotes the pressure and μ stands for the chemical potential. The symbols $\mathrm{d}E$, $\mathrm{d}S$, $\mathrm{d}V$ and $\mathrm{d}N$ represent a small change in energy, entropy, volume or particle number. Equation (2.3) makes it possible to calculate the change of internal energy in a system for changes of the state variables entropy, volume and particle number.

2.2. Second law

In thermodynamics, the second law sets the arrow of time. Consider a system and its environment that undergo a change of entropy ΔS_{sys} and ΔS_{env} during a process. It turns out that the total entropy change $\Delta S_{\mathrm{tot}} = \Delta S_{\mathrm{sys}} + \Delta S_{\mathrm{env}}$ can only be positive for isolated thermodynamic systems:

$$\Delta S_{\mathrm{tot}} \geq 0. \tag{2.4}$$

No change of entropy ($\Delta S_{\mathrm{tot}} = 0$) is only reached by reversible processes. Now, a state of equilibrium can be defined by a vanishing entropy production $\dot{S}_{\mathrm{tot}} = 0$. This formulation is sufficient in contrast to the naive definition of an equilibrium state at the start. The second law was originally not formulated in the way shown above. Historically, thermodynamics was mostly about heat engines. From that point of view, notable equivalent formulations of the second law are from Clausius [6] and Kelvin [23]. The formulation of the second law by Clausius says that, when two systems are in thermal contact without further energy exchange in form of work, the heat will only flow from the system with the higher temperature to the system with the lower temperature. Kelvin's formulation stated that, for a cyclic process, the heat absorbed by the system can not be fully converted into work.

2.3. Carnot efficiency

A very important process in thermodynamics is the Carnot process. First of all, it gives an upper bound for the thermal efficiency for heat engines according to Carnot's theorem [4]. We will later express the efficiency at maximum power of the minimal model in terms of Carnot efficiency. Therefore, a good understanding of the limits of Carnot efficiency is helpful. The Carnot process is a thermodynamic cyclic process pictured in Fig. 2.1 and exchanges heat with the environment only at two temperatures. The Carnot process can run reversible or irreversible.

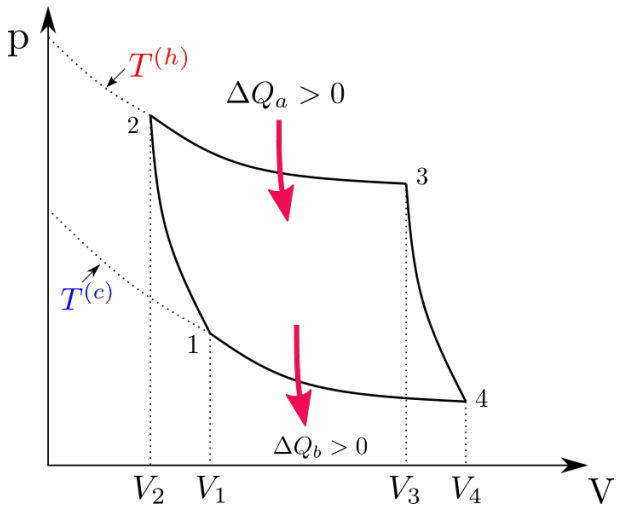

Figure 2.1.: Carnot process working with the hot reservoir at temperature T_h and the cold reservoir at temperature T_c. An amount of heat ΔQ_a and ΔQ_b is exchanged.

A path in the space of state variables can be assigned to each thermodynamic process. Reversibility is now given if a process can be stopped and the exact path in the space of state variables can be traversed in the opposite direction to the starting point. All paths of reversible processes describe a manifold and the paths of irreversible processes leave this manifold at one point.
To continue, the Carnot process can be divided into four parts:

- $1 \to 2$: adiabatic compression from a cold temperature T_c to a hot temperature T_h, with the volume changing from V_1 to V_2
- $2 \to 3$: isothermic expansion from volume V_2 to V_3 ($\Delta T = 0$)
- $3 \to 4$: adiabatic expansion from temperature T_h to T_c, with the volume changing from V_3 to V_4
- $4 \to 1$: isothermic compression from volume V_4 to V_1 ($\Delta T = 0$)

Thermal efficiency is defined as the quotient of outgoing work to incoming heat. Using the first law in Eq. (2.1a) and $\Delta Q = \Delta Q_a + \Delta Q_b$ yields the Carnot efficiency

$$\eta_c = \frac{-\Delta W}{\Delta Q_a} = 1 + \frac{\Delta Q_b}{\Delta Q_a}. \tag{2.5}$$

As the initial state is also the final state after one completion of the cycle, the entropy of the system has not changed. Therefore, the entropy changes ΔS_a and ΔS_b obey $\Delta S_a = -\Delta S_b$. When the Carnot engine is run reversible, Q_b/Q_a is independent of the working substance. Thus, the ideal gas can be chosen as a working substance and

$$\eta_c = 1 - \frac{T_c}{T_h} \tag{2.6}$$

follows with the caloric state function. As an alternative, the same expression can be calculated with the definition of the entropy in Eq. (2.2b). It can be observed that an ideal efficiency of 1 is only achieved in a Carnot process if the cold heat bath is at temperature $T_c = 0$, which is forbidden by the third law of thermodynamics. With the formulations of the second law of Clausius and Kelvin and an argument based on reversibility, it can be proven that

$$\frac{Q_c}{T_c} + \frac{Q_h}{T_h} \leq 0 \tag{2.7}$$

holds for any Carnot process. Now, any cyclic process can be approximated by a sequence of Carnot processes. This turns Eq. (2.7) into an integral

$$\oint_{\mathcal{C}} \frac{đQ}{T} \leq 0 \tag{2.8}$$

where the equality only holds if the process $\mathcal{C}$ is reversible. Any heat engine reaches a maximal and a minimum temperature while undergoing a cyclic process. For the Carnot process, the cold temperature is the minimal temperature $T_c = T_{\min}$ and the hot temperature is the maximal temperature $T_h = T_{\max}$. With the maximal and minimal temperature and splitting the integral into dispensed heat and absorbed heat, Eq. (2.8) can be estimated downwards [13]. This approach yields

$$\begin{aligned} 0 \quad &\geq \quad \oint_{\mathcal{C}} \frac{đQ}{T} = \int\limits_{đQ>0} \frac{đQ}{T} - \int\limits_{đQ<0} \frac{|đQ|}{T} \geq \frac{1}{T_{\max}} \int\limits_{đQ>0} đQ - \frac{1}{T_{\min}} \int\limits_{đQ<0} |đQ| \\ &\geq \quad \frac{Q_{\text{to}}}{T_{\max}} - \frac{|Q_{\text{from}}|}{T_{\min}} \qquad \Rightarrow \qquad \frac{|Q_{\text{from}}|}{Q_{\text{to}}} \geq \frac{T_{\min}}{T_{\max}}. \end{aligned} \tag{2.9}$$

The expression of the efficiency of any heat engine is then

$$\eta = 1 - \frac{|Q_{\text{from}}|}{Q_{\text{to}}} \leq 1 - \frac{T_{\min}}{T_{\max}} = \eta_C \tag{2.10}$$

always equal or less than the Carnot efficiency. The heat engine is only required to run on a cyclic process. Despite that, there are no other restrictions. Therefore, it is proven that the Carnot efficiency is indeed an upper bound for any heat engine.

2.4. The Curzon-Ahlborn efficiency

It was seen that the highest possible thermal efficiency is reached by a Carnot engine, which is run reversible. However, reversibility requires that the process is quasi-static. A quasi-static process runs through a sequence of equilibrium states. This means that the system has to relax to the equilibrium state before the next state in the sequence can be reached. Mathematically, quasi-stationarity is never reached in any process. In reality, a process can be in the near of quasi-stationarity if the time scale of the process is significantly larger than the time scale of the relaxation time of the system. But constructing a Carnot engine is in reality very impractical because implementing the adiabatic transitions poses a major challenge for engineers. To stay in the engineer's perspective, it is valuable to know the maximum of power that can be extracted from a heat engine. The efficiency evaluated at this point of maximum power is also of interest. Curzon and Ahlborn investigated a Carnot engine where the heat flow is modeled irreversibly with the Fourier law for heat transfer. They calculate the efficiency at maximum power for this engine and it matches surprisingly well with the efficiency of power plants in reality, see Ref. [7]. The derivation of Curzon and Ahlborn for the Carnot engine pictured in Fig. 2.1 will be illustrated shortly. During the isothermal expansion phase $2 \to 3$, the heat flux J_a

$$J_a = \alpha(T_h - T_{wh}) \tag{2.11}$$

is depending on the temperature T_h of the hot reservoir, the temperature T_{wh} of the working substance and a thermal conductivity constant α. As the isothermal expansion lasts t_1 seconds, the heat contribution to the system is

$$Q_a = J_a t_1 = \alpha t_1 (T_h - T_{wh}). \tag{2.12}$$

For the isothermal compression in phase $4 \to 1$, the dispensed heat is equal to

$$Q_b = \beta t_2 (T_c - T_{wc}), \tag{2.13}$$

where β is again a thermal conductivity constant, t_2 is the duration of the isothermal compression, T_c is the temperature of the cold reservoir and T_{wc} the temperature of the working substance. Then, it is assumed that the adiabatic compression $3 \to 4$ and expansion $1 \to 2$ take the time $(\gamma - 1)(t_1 + t_2)$, where γ is a constant larger than one. So the duration of the adiabatic processes is at least proportional to the duration of the isothermal transitions. As there is no change of internal energy, the amount of outgoing work is given by

$$-W = Q = Q_a + Q_b. \tag{2.14}$$

One finds for the power output and the efficiency

$$P = \frac{Q_a + Q_b}{(t_1 + t_2)\gamma} \tag{2.15a}$$

$$\eta = \frac{Q_a + Q_b}{Q_a}. \tag{2.15b}$$

The whole process is run reversible. While the adiabatic expansion and compression produce no entropy change, the isothermal expansion and compression lead to a change of entropy ΔS_a and ΔS_b. Because of reversibility, the entropy changes ΔS_a and ΔS_b can be written down as

$$\Delta S_a = \frac{Q_a}{T_{wh}} \tag{2.16a}$$

$$\Delta S_b = \frac{Q_b}{T_{wc}}. \tag{2.16b}$$

However, the entropy change of the system follows $\Delta S_{\text{sys}} = 0$, because it is a cyclic process. Then, the sum of $\Delta S_a + \Delta S_b$ needs to be zero

$$\Delta S_{\text{sys}} = \Delta S_a + \Delta S_b = 0. \tag{2.17}$$

Inserting Eq. (2.16b) and (2.16b) and the expressions for Q_a and Q_b in Eq. (2.12) and (2.12) yields

$$\frac{t_1}{t_2} = \frac{\beta T_{wh}(T_{wc} - T_c)}{\alpha T_{wc}(T_h - T_{wh})}. \tag{2.18}$$

Eq. (2.18) can be used to simplify the expression for power in eq. (2.15a). As a result, one gets, with introduction of the variables $x = T_h - T_{wh}$ and $y = T_{wc} - T_c$, the expression

$$P = \frac{\alpha\beta xy(T_h - T_c - x - y)}{\gamma[\beta T_h y + \alpha T_c x + xy(\alpha - \beta)]} \tag{2.19}$$

for power. The power output can now be maximized with respect to variables x and y requiring the derivatives to vanish

$$\frac{\partial P}{\partial x} = 0 \tag{2.20a}$$

$$\frac{\partial P}{\partial y} = 0. \tag{2.20b}$$

It's important to see the nature of this optimization. The temperatures T_h and T_c are assumed to be fixed. To maximize power, one can only variate the temperature of the working substance in the isothermal expansion and compression phase. The derivatives in Eq. (2.20a) and (2.20b) give conditions eliminating the variables x and y after some algebra. Finally, the so-called Curzon-Ahlborn efficiency reads

$$\eta_{CA} = 1 - \sqrt{\frac{T_c}{T_h}} = 1 - \sqrt{1 - \eta_c}. \tag{2.21}$$

An interesting thing to see is that η_{CA} does not depend on the thermal conductivities α and β and the time constant γ. The efficiency can be expressed in terms of the Carnot efficiency η_c by expanding the equation for small η_c (equilibrium)

$$\eta_{CA} = \frac{1}{2}\eta_c + \frac{1}{8}\eta_c^2 + o(\eta_c^3). \tag{2.22}$$

As we see later, the coefficient in linear order $\frac{1}{2}$ has universality for a specific class of stochastic thermodynamic machines at maximum power. Therefore, it's interesting to see that this coefficient is also a result of a macroscopic analysis of a Carnot engine at maximum power.

3. Irreversible thermodynamics

Processes in thermodynamics can be labeled as reversible and irreversible. In the space of state variables, the paths of reversible processes describe a manifold and reversibility ends when a process leaves the manifold. But how can reversibility be defined mathematically? An example of an irreversible process is the heat equation

$$\frac{1}{\alpha}\frac{\partial T}{\partial t} = \triangle T \tag{3.1}$$

which describes general heat conduction. The constant α is the thermal diffusivity and T is the temperature. When the time t is substituted with a new parameter $t' = -t$, the corresponding equation is not the heat equation. Therefore is the heat equation not invariant for the substitution $t \to t'$. Because $t \to t'$ stands for a reversal of time, heat conduction is not reversible. For irreversible processes, the arrow time is given by the second law of thermodynamics in Eq. (2.4) as the change of entropy of the environment and the system can only be positive.

3.1. The principle of microscopic reversibility

The Hamilton equations for a system without an external magnetic field or overall rotation are symmetric under time reversal. The Hamilton equations are given by

$$\frac{\mathrm{d}q_k}{\mathrm{d}t} = \frac{\partial H(q,p)}{\partial p_k} \quad \text{and} \quad \frac{\mathrm{d}p_k}{\mathrm{d}t} = -\frac{\partial H(q,p)}{\partial q_k}, \tag{3.2}$$

where $H(q,p)$ is the Hamilton function, q denotes the general coordinates and p stands for the respective conjugate momenta. The Hamilton equations stay invariant for the substitution $t \to \bar{t} = -t$, $q_k \to \overline{q}_k = q_k$ and $p_k \to \overline{p}_k = -p_k$ and therefore are invariant for time reversal. For each possible trajectory in phase space, another eligible trajectory can be found by reflecting the values of p_k and traversing it in the opposite direction, more in Ref. [26]. This also means that, in phase space, the starting point $(q_k^{\mathrm{st}}, p_k^{\mathrm{st}})$ and the end point $(q_k^{\mathrm{end}}, p_k^{\mathrm{end}})$ become $(q_k^{\mathrm{end}}, \overline{p}_k^{\mathrm{end}})$ and $(q_k^{\mathrm{st}}, \overline{p}_k^{\mathrm{st}})$ respectively after reversing time. The *principle of microscopic reversiblity* first states that microscopic dynamics of particles inherit time reversibility from the Hamilton equations. Second, it requires every process to have a reverse process and in equilibrium, the process and its reversed process take place at an equal rate. Extending the point of equal rates to macroscopic physics leads to the *principle of detailed balance*. The *Onsager reciprocal relations* are also implied by microscopic reversibility.

3.2. Thermodynamic forces, linear response and reciprocal relations

The following illustration is based on [2]. In macroscopic irreversible thermodynamics, a thermodynamic process is driven by a generalized force X which cause a response from the system in form of flux J. The force X is the change of the entropy with regard to an extensive state variable α and the flux J is the change of the state variable α with time.

$$\frac{\mathrm{d}S_{\mathrm{tot}}}{\mathrm{d}t} = \frac{\mathrm{d}S_{\mathrm{tot}}}{\mathrm{d}\alpha}\frac{\mathrm{d}\alpha}{\mathrm{d}t} = JX \quad \text{with} \quad J = \frac{\mathrm{d}S_{\mathrm{tot}}}{\mathrm{d}\alpha} \quad \text{and} \quad X = \frac{\mathrm{d}\alpha}{\mathrm{d}t} \tag{3.3}$$

Because entropy is additive, multiple sources of entropy production can be identified in a system leading to various fluxes and thermodynamic forces

$$\frac{\mathrm{d}S_{\mathrm{tot}}}{\mathrm{d}t} = \sum_i \frac{\mathrm{d}S_i}{\mathrm{d}t} = \sum_i J_i X_i \tag{3.4}$$

If the system, in which the process takes place, is at equilibrium, the thermodynamic forces vanish and the entropy production is zero. The introduced thermodynamic forces can be compared to a restoring force driving the system to the equilibrium state. Within linear response theory of macroscopic irreversible thermodynamics, the flux J is proportional to the thermodynamic force X

$$J = LX \tag{3.5}$$

with L being a constant. Consider two irreversible transport processes like heat and electrical conduction to take place in a system. The heat flux J_1 is not only dependent on the corresponding thermodynamic force X_1 but is instead also influenced by the thermodynamic force X_2 attributed to the electrical conduction. This cross-influence is widely documented. Notable examples for such a cross-dependence are the Thomson effect [23], the Peltier effect [16], and the Seebeck effect [21]. All these effects deal with an electrical current being influenced by a temperature gradient or vice-versa. Therefore, the constant L needs to be extended to a second-order tensor L

$$J_i = \sum_j L_{ij} X_j \tag{3.6}$$

where the cross-dependence is now incorporated. The elements L_{ij} are called Onsager coefficients. With the concept of microscopic reversibility and the theory of fluctuations, it was proven by Onsager [15] that the tensor L obeys the reciprocal relations

$$L_{ij} = L_{ji} \tag{3.7}$$

and is therefore symmetric. When the system is far enough away from equilibrium, the linear approximation of the fluxes with the thermodynamic forces is

not valid anymore and a local equilibrium can not be defined. A local equilibrium means that equilibrium can be assumed in a neighborhood about a point in thermodynamic space because the intensive parameters are varying slowly in space and time. Then, the reciprocal relations are invalid.

4. The master equation

To describe irreversible microscopic systems, the theory of ensembles and macroscopic irreversible thermodynamics can not be put to use. It's possible to build up a microscopic theory of irreversibility on the basis of Markovian processes. In this case, the master equation will be used to describe microscopic irreversible systems. The treatment of the master equation will be based on the description in Ref. [26].

4.1. Derivation of the master equation

The master equation can be derived from the Chapman-Kolmogorov equation for small time intervals and differentiable transition rates defined continuously in time. First, the probability distribution P of a stochastic variable X will be denoted with $P(X)$. The probability density should be nonnegative and normalized

$$P(x) \geq 0 \tag{4.1a}$$

$$\int P(x)dx = 1. \tag{4.1b}$$

The probability distribution $P(X)$ can be used to define statistical values such as average or variance. Also, the stochastic variable can be allowed to have multiple components r. Then, $P(X)$ is a function of each component $P(x_1, \ldots, x_r)$. We can also introduce a conditional probability

$$P(x_1, \ldots, x_s | x_{s+1}, \ldots, x_r), \tag{4.2}$$

which gives the probability of getting values x_1 to x_s under the condition that x_{s+1} to x_r are fixed. This leads to *Bayes' rule*, which can be formulated as

$$P(x_1, \ldots, x_s | x_{s+1}, \ldots, x_r) P(x_{s+1}, \ldots, x_r) = P(x_1, \ldots, x_r). \tag{4.3}$$

Bayes' theorem essentially says that we can get the probability $P(x_1, \ldots, x_r)$ by using the conditional probability $P(x_1, \ldots, x_s | x_{s+1}, \ldots, x_r)$ and the probability $P(x_{s+1}, \ldots, x_r)$. However, Bayes' rule is mostly used to obtain the conditional probability $P(x_1, \ldots, x_s | x_{s+1}, \ldots, x_r)$.
Finally, we can turn to stochastical processes. The stochastic variables in the case of stochastic processes can be seen as tupels (t_i, y_i), which consist of a point in time t_i and a value y_i at that point in time. Generally, the conditional

probability of a stochastic process for (t_n, y_n) is depending on all prior tupels (t_i, y_i)

$$P(y_n, t_n | y_1, t_1; \ldots, y_{n-1}, t_{n-1}). \tag{4.4}$$

A Markovian process is now defined by the requirement that the conditional probability for (t_n, y_n) should only depend on the last previous tuple (t_{n-1}, y_{n-1}). Therefore, all the other prior tuples are completely irrelevant. The process holds no memory of the other prior states. The property of Markovian processes can be expressed as

$$P(y_n, t_n | y_1, t_1; \ldots; y_{n-1}, t_{n_1}) = P(y_n, t_n | y_{n-1}, t_{n-1}), \tag{4.5}$$

The Chapman-Kolmogorov equation

$$P(y_3, t_3 | y_1, t_1) = \int P(y_3, t_3 | y_2, t_2) P(y_2, t_2 | y_1, t_1) dy_2 \tag{4.6}$$

provides an identity that needs to be obeyed by probability densities of Markovian processes. It describes that the conditional probability $P(y_3, t_3 | y_1, t_1)$ can be found by creating an intermediate point (y_2, t_2) and summing up the conditional probabilities to and from all intermediate points. If a Markovian process is stationary, the transition probability is only depending on the time interval $\tau = t_2 - t_1$ and shall therefore be written as

$$P(y_2, t_1 + \tau | y_1, t_1) = T_\tau(y_2 | y_1) \qquad \text{with} \qquad \tau = t_2 - t_1. \tag{4.7}$$

The Chapman-Kolmogorov equation can then be rewritten as

$$T_{\tau+\tau'}(y_3 | y_1) = \int T_{\tau'}(y_3 | y_2) T_\tau(y_2 | y_1) dy_2. \tag{4.8}$$

For small $\Delta\tau$ the transition probability can be approximated by

$$T_{\Delta\tau}(y_2 | y_1) = (1 - a_0 \Delta\tau)\delta(y_2 - y_1) + \Delta\tau W(y_2 | y_1) + o(\Delta\tau) \tag{4.9}$$

where $W(y_2 | y_1)$ is a transition probablity per unit time from y_1 to y_2. The coefficient $(1 - a_0\Delta\tau)$ denotes the probability that no transition occurs. The constant a_0 is therefore the probability that any transition happens, so a_0 can be calculated as

$$a_0(y_1) = \int W(y_2 | y_1) dy_2. \tag{4.10}$$

Plugging Eq. (4.9) into the Chapman-Kolmogorov equation in Eq. (4.8) for $T_{\tau'}$ yields

$$T_{\tau+\Delta\tau}(y_3 | y_1) = [1 - a_0(y_3)\Delta\tau] T_\tau(y_3 | y_1) + \Delta\tau \int W(y_3 | y_2) T_\tau(y_2 | y_1) dy_2. \tag{4.11}$$

Taking the limit $\Delta\tau \to 0$ after dividing by $\Delta\tau$ brings up the differential form

$$\frac{\partial T_\tau(y_3 | y_1)}{\partial \tau} = \int \left[W(y_3 | y_2) T_\tau(y_2 | y_1) - W(y_2 | y_3) T_\tau(y_3 | y_1) \right] dy_2, \tag{4.12}$$

which is called *master equation*. Suppose a system has a discrete amount of m microscopic states. Then, the probability density is also discrete and the master equation in Eq. (4.12) simplifies to

$$\frac{\mathrm{d}p_m}{\mathrm{d}t} = \sum_{m' \neq m} \left(W_{mm'} p_{m'} - W_{m'm} p_m \right), \tag{4.13}$$

where $W_{mm'}$ is the transition probability per unit time from state m' to m and p_m the probability to be in state m. In this form, it is apparent that the master equation is essentially a gain-loss equation as $W_{mm'} \geq 0$ is valid for $m \neq m'$. The diagonal terms $W_{mm'}$, where $m = m'$, are not contributing to a change of p_n. To sum it all up, the master equation can be used to model Markov processes in continuous time if transition rates can be defined, which requires an analytical behavior of transition probabilities for small time steps.

4.2. Properties of the master equation

A matrix $\mathbb{W}$ can be introduced as follows:

$$\mathbb{W}_{mm'} = W_{mm'} - \delta_{mm'} \sum_{m''} W_{m''m}. \tag{4.14}$$

Because the diagonal element $W_{mm'}$ vanishes, it is possible to introduce a new diagonal element containing the loss term of Eq. (4.13). The master equation then takes the form

$$\dot{p}_m(t) = \sum_{m'} \mathbb{W}_{mm'} p_{m'}(t) \tag{4.15}$$

or in compact vector-matrix notation

$$\dot{p}(t) = \mathbb{W} p(t). \tag{4.16}$$

This formulation is appealing in the sense that it does not differ much from differential equations physicists are used to deal with. It's now easy to see that the master equation is a linear differential equation of first order and has some similarity to the Schrödinger equation. However, there is a very important difference as the coefficient matrix of these two differential equations has entirely different properties. The Hamilton operator $\mathcal{H}$ is symmetric and thus can be diagonalized. A transformation into the eigenspace makes dealing with the Schrödinger equation pretty convenient. In contrast, the matrix $\mathbb{W}$ does not need to be symmetric but has the two properties

$$\mathbb{W}_{mm'} \geq 0 \quad \text{for } m \neq m' \tag{4.17a}$$

$$\sum_{m} \mathbb{W}_{mm'} = 0 \quad \text{for each } m'. \tag{4.17b}$$

Equation (4.17a) states that off-diagonal elements are nonnegative. This stems from the fact that the off-diagonal elements are transition probabilities. Equation (4.17a) is not valid for the diagonal element, because it was introduced as a negative sum of positive transition probabilities. Furthermore, Eq. (4.17b) incorporates the fact that probability has to be conserved. Following Ref. [26], a matrix will be called a $\mathbb{W}$-matrix when Eq. (4.17a) and (4.17b) apply. It can be seen from Eq. (4.17b) that a $\mathbb{W}$-matrix always has the left eigenvector $(1, \ldots, 1)$ with zero eigenvalue. Linear Algebra then also requires a $\mathbb{W}$-matrix to have a right eigenvector with eigenvalue zero. In the context of stochastical thermodynamics, this right eigenvector is called steady-state solution p_{ss} of the master equation and is determined by

$$\mathbb{W}\, p_{ss} = 0. \tag{4.18}$$

The steady-state solution is a key point in dealing with irreversible thermodynamic processes and will be subject to the rest of this work. It will be also be proven that the master equation is asymptotic stable. Any initial probability distribution p will relax into the steady-state solution. This justifies the focus on this steady-state solution, which will serve as a basis for the later introduced stochastical thermodynamics.

4.3. Relaxation towards the stationary solution and uniqueness

In the prior section, the master equation was derived from a Markovian process. And it was shown that at least one stationary solution exists. However, it's not a trivial question whether or not this stationary solution is even a probability distribution, let alone stable. What does it matter when irreversible thermodynamics can be treated in the regime of the steady-state solution, but this solution is never reached or unstable? The Uniqueness of the stationary solution is an important property. This means that the stationary solution given by Eq. (4.18) is the only stationary solution possible. Relaxation towards the stationary solution means that any arbitrary starting condition tends towards the stationary solution for $t \to \infty$

$$p_n(t) - p_{\mathrm{ss}} \xrightarrow{t\to\infty} 0. \tag{4.19}$$

Uniqueness and relaxation will be proven with Ref. [26]. However, there are multiple different approaches, e.g. Ref. [19], which uses network theory and Lyapunov stability. It is assumed that $\phi(t)$ is any arbitrary solution of the master equation with states n. For each state n at a time t, the components of $\phi(t)$ can be sorted after positivity, negativity or equality to zero and be assigned

an index u, v, w:

$$\begin{aligned} \phi_n^{(u)}(t) > 0, \qquad & u \in \mathcal{U} \\ \phi_n^{(v)}(t) < 0, \qquad & v \in \mathcal{V} \\ \phi_n^{(w)}(t) = 0, \qquad & w \in \mathcal{W} \end{aligned}$$

By using the definition of a $\mathbb{W}$-matrix, the derivation in time of the arbitrary solution $\phi(t)$ can be evaluated to be zero:

$$\sum_n \dot{\phi}_n(t) = \sum_n \sum_{n'} \mathbb{W}_{nn'} \phi_{n'} = \sum_{n'} \phi_{n'} \sum_n \mathbb{W}_{nn'} = 0 \tag{4.20}$$

The sum of all positive and negative terms can be defined as $U(t)$ and $V(t)$

$$U(t) = \sum_u \phi_u(t) \qquad V(t) = \sum_v \phi_v(t) \tag{4.21}$$

The first investigation concerns the change of $U(t)$ with time. For the intervals, where no terms enter the sum $U(t)$, the change $\dot{U}(t)$ can be written as

$$\begin{aligned} \dot{U}(t) &= \sum_u \dot{\phi}_u = \sum_u \left(\sum_{u'} \mathbb{W}_{uu'} \phi_{u'} + \sum_{v'} \mathbb{W}_{uv'} \phi_{v'} \right) \\ &= \sum_{u'} \left(-\sum_v W_{vu'} - \sum_w W_{wu'} \right) \phi_{u'} + \sum_{v'} \left(\sum_u W_{uv'} \right) \phi_{v'}. \end{aligned} \tag{4.22}$$

To arrive at Eq. (4.22), one can use the property of a stochastical matrix in Eq. (4.17b), because the sums over u' and u and over u and v can be switched:

$$\begin{aligned} \sum_n \mathbb{W}_{n,u'} &= 0 = \sum_u \mathbb{W}_{u,u'} + \sum_v \mathbb{W}_{v,u'} + \sum_w \mathbb{W}_{w,u'} \\ \sum_u \mathbb{W}_{u,u'} &= -\sum_v \mathbb{W}_{v,u'} - \sum_w \mathbb{W}_{w,u'} = -\sum_v W_{v,u'} - \sum_w .W_{w,u'} \end{aligned}$$

For the other sum follows

$$\sum_u \mathbb{W}_{u,v'} = \sum_u W_{u,v'}.$$

Note that summing over u is not the same as summing over n in Eq. (4.17b). It can be seen in Eq. (4.22) that

$$\dot{U}(t) \leq 0 \tag{4.23}$$

holds for time intervals, where no term enters U, as the sum only consists of negative terms. For the points in time, where terms enter the sum, U is not differentiable but still continuous. Therefore, U is continuous for all times t. Because the inequality in Eq. (4.23) is only broken for discrete points in time and U is continuous for all times t, the sum $U(t)$ can not increase. In Eq. (4.20), it was shown that the probability distribution $\sum_n \phi_n(t)$ is conserved in time. Therefore, the sum $U(t)+V(t)$ is also constant. The sum $U(t)$ is non-increasing ($\dot{U}(t) \leq 0$), so the sum $V(t)$ has to be non-decreasing ($\dot{V}(t) \geq 0$). This leads to an interesting fact.

Corollary 1. *If $\phi_n(0) \geq 0$ for all n, then $\phi_n(t) \geq 0$ for all n*

If $\phi_n(0) \geq 0$ for all n, then $\phi_n(0) < 0$ holds for no n. Then, the set $\mathcal{V}$ has to be empty and $V(0) = 0$ is valid. As the sum V is non-decreasing $\dot{V}(t) \geq 0$, it has to stay empty for all times t. If the initial condition $\phi(0)$ is a probability distribution which is is non-negative ($\phi(0) \geq 0$), then the arbitrary solution $\phi(t)$ will stay non-negative for all times t. The corollary ensures that once a probability distribution is chosen as an initial state, the solution will also consist of probability distributions.

The second part of the proof can not be illustrated accurately in this context. However, the general idea is to assume that the system described by the master equation is a typical microscopic system. The system should not consist of two subsystems and splitting subsystems, where probability is absorbed by one system. Two subsystems connected by one edge only passable in one direction are also excluded. Equation (4.23) makes sure that $U(t)$ converges for the limit $t \to \infty$ to a value $U(\infty) \geq 0$ as $U(t)$ is by definition non-negative. The same argument can be made for $V(\infty)$. For convergence, it is important that both $\dot{U}(\infty) = \dot{V}(\infty) = 0$ vanish. The arbitrary solution starts with an initial value C

$$\sum_n \phi_n(0) = C = const. \tag{4.24}$$

Next, the following corollary postulates that all terms of the arbitrary solution will ultimately have the same sign.

Corollary 2. *The terms of a solution ϕ_n are strictly non-negative or non-positive for $t \to \infty$ meaning either $\phi_n(\infty) \geq 0$ or $\phi_n(\infty) \leq 0 \quad \forall n$*

If it's proven that for a $C \geq 0$ the sum $V(\infty) = 0$ or for a $C \leq 0$ the sum $U(\infty) = 0$ vanishes, then all terms of $\phi_n(t)$ will have the same sign ultimately. This can be proven with an argument about typical microscopic systems. The corollary is important because then a probability distribution can be a stationary solution $\phi(\infty)$ of the master equation.

A stationary probability distribution p^s has non-negative components and the sum of all states is $C = 1$. Imagine two probability distributions $p_n^{(1)}$ and $p_n^{(2)}$ governed by the master equation. Because of linearity, the superposition is also a solution of the master equation

$$\phi_n = p_n^{(1)} - p_n^{(2)} \quad \text{with} \quad C = 0. \tag{4.25}$$

It's seen that for $C = 0$ all terms of ϕ_n have to vanish because U is non-increasing and V is non-decreasing. Then, the two solutions are equal

$$\phi_n = p_n^{(1)} - p_n^{(2)} \xrightarrow{t\to\infty} 0. \tag{4.26}$$

It's now clear that only one time-independent stationary probability distribution exists. And this stationary distribution is also attractive for every probability distribution as an initial distribution.

4.4. The principle of detailed balance

The principle of detailed balance was first proposed by Boltzmann to prove his famous H-Theorem. When the transition probabilities $W_{m,m'}$ and $W_{m',m}$ obey a balance equation with regard to the equilibrium occupation probabilities p_m^{eq} and $p_{m'}^{eq}$

$$W_{m,m'} p_{m'}^{eq} = W_{m',m} p_m^{eq}., \tag{4.27}$$

then the occupation probabilities p_m will tend for $t \to \infty$ towards the equilibrium occupation probability for that state. The equilibrium occupation probabilities are given by the ensemble theory. The principle of detailed balance can be seen as microscopic reversibility since each process has the same non-conditional probability to take place as its inverse process in the equilibrium state. In fact, demanding microscopic reversibility is sufficient enough to derive the principle of detailed balance.

5. Stochastic thermodynamics

This chapter is primarly based on elobarations from van den Broek, see Ref. [25]. Stochastic thermodynamics is introduced by an example of a system governed by a master equation in contact with ν heat and particle reservoirs. Because the system is described by a master equation, irreversibility is built in from the start. An energy ε_m, an occupation probability p_m and a time-independent particle number n_m are assigned to each state m. The average energy and the average particle number can be calculated by

$$\varepsilon = \sum_m \varepsilon_m p_m \tag{5.1}$$

$$n = \sum_m n_m p_m. \tag{5.2}$$

A probability flux $J_{m,m'}$ can be introduced as

$$J_{m,m'} = W_{m,m'} p_{m'} - W_{m',m} p_m \tag{5.3}$$

with $W_{m,m'}$ and $W_{m',m}$ being the transition probabilities between the states m and m'. The master equation in Eq. (4.13) can then be written as

$$\frac{\mathrm{d}p_m}{\mathrm{d}t} = \sum_{m'} J_{m,m'}, \tag{5.4}$$

where the sum on the right is the total probability flux to state m (including gain and loss terms). To simplify the notation, the energy and particle differences $\varepsilon_{m,m'}$ and $n_{m,m'}$ are defined as

$$\varepsilon_{m,m'} = \varepsilon_m - \varepsilon_{m'} \tag{5.5}$$

$$n_{m,m'} = n_m - n_{m'}. \tag{5.6}$$

The system is in contact with a number ν of heat and particle reservoirs. Each reservoir is in equilibrium at a temperature $T^{(\nu)}$ and chemical potential $\mu^{(\nu)}$. To further build up the theory, it is assumed that each reservoir contributes an additive term to the total transition matrix $\mathbb{W}$

$$\mathbb{W} = \sum_\nu \mathbb{W}^{(\nu)}. \tag{5.7}$$

This assumption seems plausible because the master equation is linear. Then, it follows that also the probability flux $J_{m,m'}$ consists of additive terms from each reservoir

$$J_{m,m'} = \sum_\nu J^{(\nu)}_{m,m'}. \tag{5.8}$$

An energy, particle and heat change can be attributed to a reservoir ν

$$\dot{E}^{(\nu)} = \frac{1}{2} \sum_{m,m'} \varepsilon_{m,m'} J^{(\nu)}_{m,m'} \tag{5.9}$$

$$\dot{N}^{(\nu)} = \frac{1}{2} \sum_{m,m'} n_{m,m'} J^{(\nu)}_{m,m'} \tag{5.10}$$

$$\dot{Q}^{(\nu)} = \frac{1}{2} \sum_{m,m'} q^{(\nu)}_{m,m'} J^{(\nu)}_{m,m'}. \tag{5.11}$$

The factor 1/2 arrises when $\dot{E}$, $\dot{N}$ and $\dot{Q}$ are written in the compact notation $\varepsilon_{m,m'}$ and $n_{m,m'}$, but can always be switched with a sum over m and m' with the condition $m > m'$. In Eq. (5.11), the difference between energy and chemical work is written as a heat contribution from reservoir ν in accordance with the first law. The heat contribution $q^{(\nu)}_{m,m'}$ is defined as

$$q^{(\nu)}_{m,m'} = \varepsilon_{m,m'} - \mu^{(\nu)} n_{m,m'} \tag{5.12}$$

The chemical work contribution of each reservoir is given by

$$\dot{W}^{(\nu)}_{\text{chem}} = \mu^{(\nu)} \dot{N}^{(\nu)} = \frac{1}{2} \sum_{m,m'} \mu^{(\nu)} n_{m,m'} J^{(\nu)}_{m,m'}. \tag{5.13}$$

5.1. Entropy production

In the context of stochastic thermodynamics, the Shannon entropy is used. This definition of entropy is named after Shannon, see Ref. [22], and agrees in equilibrium with statistical physics. It's verified by plugging in the probability from ensemble theory. Then, the corresponding differential can be derived. The Shannon entropy for the system is

$$S_{\text{sys}} = -k_{\text{B}} \sum_{m} p_m \ln p_m \tag{5.14}$$

where k_{B} is the Boltzmann constant and p_m denotes the probability to be in state m. Now, the entropy production can be investigated. Two separate parts can be identified in the entropy production. As illustrated in Ref. [25], the

entropy change of the system can be written as

$$\begin{aligned}
\frac{\mathrm{d}S_{\mathrm{sys}}}{\mathrm{d}t} &= - k_{\mathrm{B}} \sum_m \frac{\mathrm{d}p_m}{\mathrm{d}t} \ln(p_m) - k_B \sum_m \frac{\mathrm{d}p_m}{\mathrm{d}t} \\
&= - k_B \sum_m \frac{\mathrm{d}p_m}{\mathrm{d}t} \ln(p_m) - k_B \frac{\mathrm{d}}{\mathrm{d}t} \sum_m p_m \\
&= - k_{\mathrm{B}} \sum_{m,m',\nu} \mathbb{W}^{(\nu)}_{m,m'} p_{m'} \ln(p_m) \\
&= - \frac{k_{\mathrm{B}}}{2} \sum_{m,m',\nu} \left[\mathbb{W}^{(\nu)}_{m,m'} p_{m'} \ln(p_m) + \mathbb{W}^{(\nu)}_{m',m} p_m \ln(p_{m'}) \right] \\
&= - \frac{k_{\mathrm{B}}}{2} \sum_{m,m',\nu} \Big[\left(W^{(\nu)}_{m,m'} p_{m\prime} - W^{(\nu)}_{m',m} p_m \right) \ln(p_m) \\
&\quad + \left(W^{(\nu)}_{m',m} p_m - W^{(\nu)}_{m,m\prime} p_{m'} \right) \ln(p_{m'}) \Big] \\
&= \frac{k_{\mathrm{B}}}{2} \sum_{m,m',\nu} \left(W^{(\nu)}_{m,m'} p_{m\prime} - W^{(\nu)}_{m',m} p_m \right) \ln \frac{p_{m'}}{p_m} \\
&= \frac{k_{\mathrm{B}}}{2} \sum_{m,m',\nu} \left(W^{(\nu)}_{m,m'} p_{m\prime} - W^{(\nu)}_{m',m} p_m \right) \ln \frac{W^{(\nu)}_{m,m'} p_{m'}}{W^{(\nu)}_{m',m} p_m} \\
&\quad + \frac{k_{\mathrm{B}}}{2} \sum_{m,m',\nu} \left(W^{(\nu)}_{m,m'} p_{m\prime} - W^{(\nu)}_{m',m} p_m \right) \ln \frac{W^{(\nu)}_{m',m}}{W^{(\nu)}_{m,m'}}
\end{aligned} \tag{5.15}$$

where the master equation was inserted in the third line. From the fourth to the fifth line, the definition of the $\mathbb{W}$ matrix in Eq. (4.14) was used and the diagonal element was written out. At first glance, it's not easy to see why Eq. (5.15) is a useful way of decomposing the entropy production into two additive terms. The advantage of writing the entropy production this way is that the probability flux can be inserted

$$\frac{\mathrm{d}S_{\mathrm{sys}}}{\mathrm{d}t} = \frac{k_{\mathrm{B}}}{2} \sum_{m,m',\nu} J^{(\nu)}_{m,m'} \ln \frac{W^{(\nu)}_{m,m'} p_{m'}}{W^{(\nu)}_{m',m} p_m} + \frac{k_{\mathrm{B}}}{2} \sum_{m,m',\nu} J^{(\nu)}_{m,m'} \ln \frac{W^{(\nu)}_{m',m}}{W^{(\nu)}_{m,m'}}. \tag{5.16}$$

Ultimately, the entropy change of the system is depending on the probability flux, which is zero in equilibrium, and on the quotient of the transition rates and the occupation probability. With the detailed balance condition, the second part of Eq. (5.16) reveals that

$$\ln \frac{W^{(\nu)}_{m',m}}{W^{(\nu)}_{m,m'}} = \ln \frac{p^{\mathrm{eq},\nu}_{m'}}{p^{\mathrm{eq},\nu}_{m}} = \beta^{(\nu)} (\varepsilon_{m,m'} - \mu^{(\nu)} n_{m,m'}) = \beta^{(\nu)} q^{(\nu)}_{m,m'} \tag{5.17}$$

can be viewed as a heat contribution from a reservoir ν. One can therefore associate the second part of Eq. (5.16) with the negative entropy exchange in

the environment,

$$-\frac{\mathrm{d}S_{\mathrm{env}}}{\mathrm{d}t} = \frac{k_{\mathrm{B}}}{2} \sum_{m,m',\nu} \beta^{(\nu)} J^{(\nu)}_{m,m'} q^{(\nu)}_{m,m'} = \sum_{\nu} \frac{\dot{Q}^{(\nu)}}{T^{(\nu)}}. \tag{5.18}$$

Then, the first part of Eq.(5.16) resembles the total entropy change with

$$\frac{\mathrm{d}S_{\mathrm{tot}}}{\mathrm{d}t} = \frac{\mathrm{d}S_{\mathrm{sys}}}{\mathrm{d}t} + \frac{\mathrm{d}S_{\mathrm{env}}}{\mathrm{d}t}. \tag{5.19}$$

In analogy to macroscopic non-equilibrium thermodynamics, the total entropy production can be written as a product of thermodynamic forces and the probability fluxes

$$\frac{\mathrm{d}S_{\mathrm{tot}}}{\mathrm{d}t} = \frac{1}{2} \sum_{m,m',\nu} J^{(\nu)}_{m,m'} X^{(\nu)}_{m,m'} \quad \text{with} \quad X^{(\nu)}_{m,m'} = k_{\mathrm{B}} \ln \frac{W^{(\nu)}_{m,m'} p_{m'}}{W^{(\nu)}_{m',m} p_m}. \tag{5.20}$$

In accordance with macroscopic irreversible thermodynamics, the defined thermodynamic forces are zero in equilibrium. Entropy is only produced when the system is not in equilibrium and $W^{(\nu)}_{m,m'} p_{m'} \neq W^{(\nu)}_{m',m} p_m$ holds. Surprisingly, the definition of entropy production is valid for any state of the system, even states nowhere near equilibrium or the linear response regime. All in all, the entropy production is in close analogy to macroscopic non-equilibrium thermodynamics which justifies the use of the Shannon entropy.

5.2. System in contact with two reservoirs

The later studied minimal model is in contact with two reservoirs. As a foundation, a system in contact with two reservoirs and with strong coupling is discussed. During the discussion, the variables $x^{(c)}$ and $x^{(h)}$ will be defined as an effective thermodynamic force and we will bring these definitions over to the minimal model. Therefore, the discussion helps with understanding the background of $x^{(c)}$ and $x^{(h)}$.

In Fig. 5.1, a system with entropy S, energy E and particle number N is in contact with two reservoirs. The energy scale is adjusted to E/k_{B}, so k_{B} can be treated as 1. The left reservoir is at a temperature $T^{(c)}$ with chemical potential $\mu^{(c)}$ and the right reservoir is at a temperature $T^{(h)}$ with chemical potential $\mu^{(h)}$. From each reservoir, there is a heat flow $\dot{Q}^{(\nu)}$ and a particle flow $\dot{N}^{(\nu)}$. The right reservoir is hotter than the left reservoir, meaning $T^{(h)} > T^{(c)}$. In classical thermodynamics, the difference in the temperature of the reservoirs can be used to do work. In this case, it can be used to transfer particles from one reservoir to the other. In stochastic thermodynamics, the system is governed by a master equation and therefore relaxes to the stationary solution at long times. The entropy production of the system $\dot{S}_{sys}$ and the energy change $\dot{E}$ is zero because it is a steady-state (entropy and energy are state functions). Also, the number of

Figure 5.1.: A representation of a system in contact with two reservoirs. The system has an entropy S, an energy E and a particle number N. Both reservoirs have a chemical potential $\mu^{(\nu)}$ and a temperature $T^{(\nu)}$. Heat and particles flow from the reservoirs to the system. The left reservoir is assumed to have a lower temperature than the right reservoir ($T^{(c)} < T^{(h)}$).[25]

particles in the system has to stay constant, which requires the particle flow to be zero $\dot{N} = 0$. Being in a steady-state implies that there is no driving force and also no work contribution $\dot{W}$ (excluding chemical work). Otherwise, it would lead to a change of occupation probability. The steady-state has not to be an equilibrium state because a difference in temperature or in chemical potential is compatible with the stationary solution. Combining the points above leads to

$$\dot{E} = \dot{N} = \dot{S}_{sys} = \dot{W} = 0. \tag{5.21}$$

The energy flow $\dot{E}$ and the particle flow $\dot{N}$ consist of contributions from each reservoir

$$\dot{E} = \dot{E}^{(c)} + \dot{E}^{(h)} = J_E^{(c)} + J_E^{(c)} \tag{5.22}$$

$$\dot{N} = \dot{N}^{(c)} + \dot{N}^{(h)} = J_N^{(c)} + J_N^{(c)}. \tag{5.23}$$

Here, the notation $J_E^{(\nu)} = \dot{E}^{(\nu)}$ and $J_N^{(\nu)} = \dot{N}^{(\nu)}$ is introduced. A preferred perspective is indicated by naming $J_E = J_E^{(c)}$ and $J_N = J_N^{(c)}$. This should illustrate that the focus lays on the energy and particle flow of reservoir one. Focusing on one particle and energy flow is possible because we look at the steady-state. Then, it's found that

$$J_E = J_E^{(c)} = \dot{Q}^{(c)} + \mu^{(c)}\dot{N}^{(c)} = \dot{E}^{(c)} = -J_E^{(h)} = -\dot{Q}^{(h)} - \mu^{(h)}\dot{N}^{(h)} = \dot{E}^{(h)} \tag{5.24}$$

$$J_N = J_N^{(c)} = \dot{N}^{(c)} = -J_N^{(h)} = \dot{N}^{(h)}. \tag{5.25}$$

The total entropy production can be attributed to the reservoirs according to Eq. (5.19) and Eq. (5.21). With Eq. (5.18) follows for the steady-state that

$$\frac{\mathrm{d}S_{\mathrm{tot}}}{\mathrm{d}t} = \frac{\mathrm{d}S_{\mathrm{env}}}{\mathrm{d}t} = -\frac{\dot{Q}^{(c)}}{T^{(c)}} - \frac{\dot{Q}^{(h)}}{T^{(h)}} \quad \text{with} \quad \dot{S}_{\mathrm{sys}} = 0 \tag{5.26}$$

The total entropy production can be rewritten with Eq. (5.24) as a product of thermodynamic forces and the energy and particle flux

$$\frac{\mathrm{d}S_{\mathrm{tot}}}{\mathrm{d}t} = J_E X_E + J_N X_N \tag{5.27}$$

$$X_E = \frac{1}{T^{(h)}} - \frac{1}{T^{(c)}} \tag{5.28}$$

$$X_N = \frac{\mu^{(c)}}{T^{(c)}} - \frac{\mu^{(h)}}{T^{(h)}}. \tag{5.29}$$

It takes exactly the form that is known from macroscopic irreversible thermodynamics. For specific systems, the particle flux J_N is proportional to the energy flow J_E with $J_E = \varepsilon J_N$, where ε is an arbitrary constant except $\varepsilon \neq 0$. If $\varepsilon > 0$ holds, energy and particles flow in the same direction. When $\varepsilon < 0$ is valid, the particle flow J_N and energy flow J_E have a different sign and therefore a different direction. The proportionality of energy and particle flux is called strong coupling, Ref. [25, 8]. With strong coupling, Eq. (5.27) reduces to

$$\frac{\mathrm{d}S_{\mathrm{tot}}}{\mathrm{d}t} = JX \quad \text{with} \quad J = J_N \quad \text{and} \quad X = X_E + \frac{X_N}{\varepsilon} \tag{5.30}$$

There is only one effective thermodynamic force X. Notably, the forces X_E and X_N do not need to be zero to have no total entropy production. With the definition of the variables $x^{(\nu)}$ as

$$x^{(\nu)} = \frac{\varepsilon - \mu^{(\nu)}}{T^{\nu}}\,, \tag{5.31}$$

it follows for the single collapsed force X

$$X = \frac{x^{(h)} - x^{(c)}}{\varepsilon}. \tag{5.32}$$

No entropy is therefore produced, when $x^{(c)} = x^{(h)}$. With the introduction of the variables $x^{(\nu)}$, symmetry is restored, because $x^{(c)}$ and $x^{(c)}$ are both weighted with $1/\varepsilon$. In this context of strong coupling, the variables $x^{(\nu)}$ can be compared to a thermodynamic force. The chemical work done by a system (without requiring strong coupling) can be written as

$$\dot{W}_{\mathrm{chem}} = \mu^{(c)} J_N^{(c)} + \mu^{(h)} J_N^{(h)} = (\mu^{(c)} - \mu^{(h)}) J_N \tag{5.33}$$

$$= (-T^{(c)} x^{(c)} + T^{(h)} x^{(h)}) J_N = T^{(h)} (x^{(h)} - (1 - \eta_c) x^{(c)}) J_N \tag{5.34}$$

with η_c being the Carnot efficiency $\eta_c = 1 - T^{(c)}/T^{(h)}$. The efficiency can now be defined as the outgoing chemical work in relation to the incoming heat from the hot reservoir

$$\eta = \frac{-\dot{W}_{\mathrm{chem}}}{\dot{Q}^{(h)}} = \frac{-T^{(h)}(x^{(h)} - (1 - \eta_c) x^{(c)}) J_N}{-J_E + \mu^{(h)} J_N} = \frac{T^{(h)}(x^{(h)} - (1 - \eta_c) x^{(c)})}{\frac{J_E}{J_N} - \mu^{(h)}}. \tag{5.35}$$

With the condition of strong coupling, the efficiency simplifies to

$$\eta = 1 - (1 - \eta_c)\frac{x^{(c)}}{x^{(h)}}. \tag{5.36}$$

Here, it is interesting to see that, when $x^{(c)} = x^{(h)}$, the corresponding efficiency is the Carnot efficiency. And since $x^{(c)} = x^{(h)}$ implies no total entropy production and therefore reversibility, the system works with Carnot efficiency exactly when it is reversible.

6. Investigation of a minimal model

In the rest of this work, a minimal model governed by a master equation will be investigated. The system is in contact with two reservoirs and is able to exchange energy and particles with the reservoirs. Symmetries of the Onsager coefficients were studied earlier, see Ref. [2]. The Onsager matrix is indeed symmetric beyond the equilibrium state for a special condition. A missing point in earlier investigated models is that there is no room for particle interactions. All of the studied systems satisfy the strong coupling property, but strong coupling is an idealization. The more realistic minimal model extends the quantum dot and adds particle interaction with an interaction energy u. With the introduction of particle interaction, the strong coupling property is broken. The exciting question of this work is how the interaction energy u and interaction in general influence maximum power and the efficiency at maximum power of the illustrated minimal model. Furthermore, the efficiency at maximum power can be expanded into terms of Carnot efficiency. The Curzon-Ahlborn efficiency was derived in Sec. 2.4, and, to reiterate, is given by

$$\eta_{\mathrm{CA}} = 1 - \sqrt{1 - \eta_c}, \tag{6.1}$$

where η_c is the Carnot efficiency. An expansion of this expression yields

$$\eta_{CA} = \frac{1}{2}\eta_c + \frac{1}{8}\eta^2 + \mathcal{O}(\eta_c^3). \tag{6.2}$$

The Curzon-Ahlborn efficiency agrees with the measured efficiencies of real power plants, see Ref. [7]. But, it's a result of macroscopic thermodynamics. Interestingly, when the focus of the investigation is shifted towards microscopic thermodynamic machines, an analysis of the efficiency at maximum power with stochastic thermodynamics yields almost the same expansion of the efficiency. In Ref. [8], a quantum dot was investigated. The system structure of a quantum dot is very simple as there are only two states and no particle interaction. For a quantum dot, an expansion of the efficiency at maximum power takes the form

$$\eta = \frac{1}{2}\eta_c + \frac{1}{8}\eta_c^2 + \mathcal{O}(\eta_c^3). \tag{6.3}$$

The expansion of the efficiency agrees with the Curzon-Ahlborn efficiency. Next, it was proven for systems satisfying the strong coupling property that the linear coefficient $\frac{1}{2}$ is universal, see Ref. [9]. Universality can be extended to the coefficient $\frac{1}{8}$ when the system has a left-right symmetry, also see Ref. [9]. Another finding from linear irreversible thermodynamics is that the linear coefficient is

bounded between $\frac{1}{2}$ and 0 for thermodynamic machines in the linear response regime, Ref. [24]. So, the efficiency at maximum power and the boundaries of the expansion seem to be well investigated. Nonetheless, microscopic systems not satisfying the strong coupling property have not been subject to a an investigation. A main concern should be answering the question if an expansion of the efficiency at maximum power takes the same form as in Eq. (6.2) and Eq. (6.3).

6.1. The minimal model

The system is in contact with two reservoirs at temperature $T^{(c)}$ and $T^{(h)}$ and the chemical potentials $\mu^{(c)}$ and $\mu^{(h)}$. The energy scale is adjusted to E/k_{B}, so k_{B} can be treated as 1. A quick summary of the three different states is given

	Energy	Particle number
State 0	0	$n = 0$
State 1	ε	$n = 1$
State 2	$2\varepsilon + u$	$n = 2$

Table 6.1.: Energies and particle numbers of the three different states.

in Tab. 6.1. Additionally, the minimal is illustrated in Fig. 6.1. In state 0, no particle is in the system and the energy is 0. With state 1, one particle is in the system and the energy of the system is ε. In state 2, two particles are in the system having the energy $2\varepsilon + u$, where u is the interaction energy. The system is able to exchange energy and particles with the reservoirs. The probability for a transition from state m' to m is given by

$$W^{(\nu)}_{m,m'} = \frac{\alpha}{1 + \exp\big(\beta^{(\nu)}(\varepsilon_{m,m'} - \mu^{(\nu)} n_{m,m'})\big)} \tag{6.4}$$

with α being a constant and $\beta^{(\nu)}$ being the inverse thermal energy, $\beta^{(\nu)} = 1/k_{\mathrm{B}}T^{(\nu)}$. These so-called "Glauber" rates were first introduced by Glauber, see Ref. [10]. The notation of $\varepsilon_{m,m'}$ and $n_{m,m'}$ was introduced in Eq. (5.5) and Eq. (5.6). The constant α is in general called an "attempt frequency". For the sake of simplicity, α will be set to 1. A transition from state 0 to state 2 or vice-versa is forbidden. For the inverse transition from state m to m', the transition probabilities obey

$$W^{(\nu)}_{m',m} = 1 - W^{(\nu)}_{m,m'}. \tag{6.5}$$

The transition rates need to be in agreement with properties at equilibrium. Therefore, a partial detailed balance is required with regards to the grand canonical distribution

$$\frac{W^{(\nu)}_{m',m}}{W^{(\nu)}_{m,m'}} = \exp\Big(\beta^{(\nu)}[\varepsilon_{m,m'} - \mu^{(v)} n_{m,m'}]\Big). \tag{6.6}$$

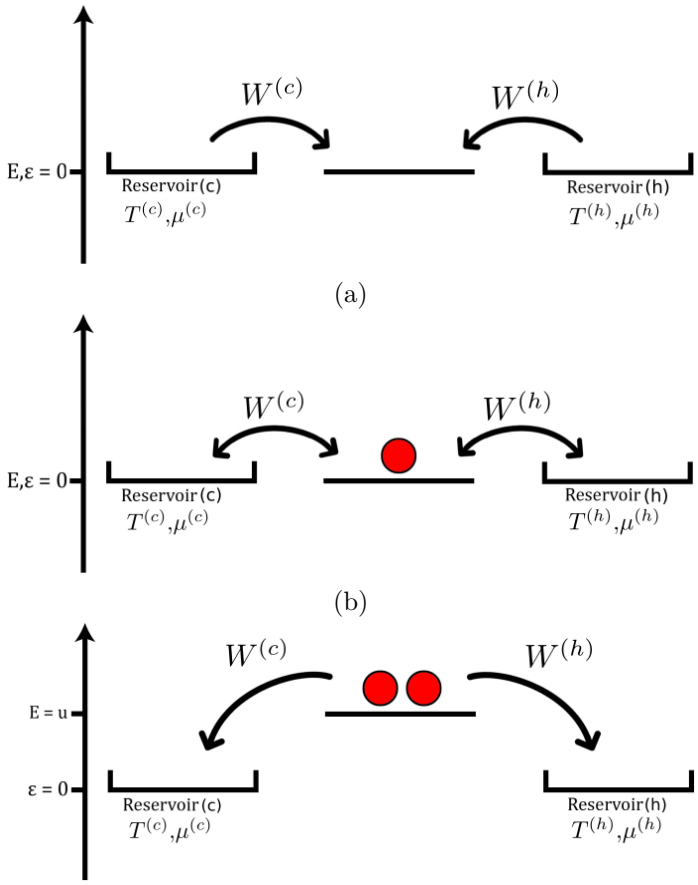

Figure 6.1.: The minimal model is in contact with two reservoirs. The left reservoir is at a temperature $T^{(c)}$ and chemical potential $\mu^{(c)}$ and the right reservoir is at a temperature $T^{(h)}$ and chemical potential $\mu^{(h)}$. The temperatures obey $T^{(c)} < T^{(h)}$. So, the left is the cold reservoir and the right is the hot reservoir. In (a), (b) and (c), the energy ε is set to 0 just for simplification. In (a), the minimal model is illustrated in state 0. No particle is in the system, but one particle can transition from the reservoirs into the system. Figure (b) shows the system in state 1. The particle in the system can either transition back into the reservoirs or another particle from the reservoirs comes into the system. In (c), the minimal is illustrated in state 2. Two particles are in the system. The interaction energy u is added on top of the energy 2ε. When the minimal model is in state 2, one particle can only transition into the reservoirs. The figure was taken from [2] and adapted.

Details can be found in Ref. [9]. When the interaction energy $\hat{u}$ is zero, the minimal model is a twofold quantum dot, which has the same properties as the regular quantum dot studied in Ref. [8]. For large positive energy barriers $\varepsilon_{m,m'} \gg 0$ the transition probability tends to 0. The minimal model is then turning into a regular quantum dot because state 2 is entirely blocked and has no relevance. For negative energy barriers $\varepsilon_{m,m'} \ll 0$, the transition probability $W_{2,1}^{(\nu)}$ becomes 1. In the high-temperature regime, all transition probabilities converge to $\frac{1}{2}$. A positive interaction energy u makes the transition from state 0 to state 1 more likely as the transition from state 1 to state 2, which means $W_{1,0}^{(\nu)} > W_{2,1}^{(\nu)}$. This implies $W_{0,1}^{(\nu)} < W_{1,2}^{(\nu)}$ for the inverse transitions. Therefore, a positive u hinders a transition into state 2 and enforces the transition to state 1 (from state 2). When the interaction energy is negative instead, the transition probabilities obey $W_{1,0}^{(\nu)} < W_{2,1}^{(\nu)}$ and therefore $W_{0,1}^{(\nu)} > W_{1,2}^{(\nu)}$. A transition into state 2 is enforced and a transition into state 1 (from state 2) is hindered.

It is also useful to introduce the thermodynamic variables $x^{(c)}$ and $x^{(h)}$ as illustrated in Sec. 5.2 with

$$x^{(c)} = \frac{\varepsilon - \mu^{(c)}}{T^{(c)}} \tag{6.7}$$

$$x^{(h)} = \frac{\varepsilon - \mu^{(h)}}{T^{(h)}}. \tag{6.8}$$

A combination of ε, $\mu^{(\nu)}$ and $T^{(\nu)}$ into one parameter $x^{(\nu)}$ is a contraction of the space of ε, $\mu^{(\nu)}$ and $T^{(\nu)}$. The point of maximum power might be described by curve for different u in the space of $x^{(c)}$ and $x^{(h)}$. In the space of ε, $\mu^{(\nu)}$ and $T^{(\nu)}$, this curve is decompressed into a manifold of a higher dimension. So, by varying the combined variables $x^{(c)}$ and $x^{(h)}$, the parameters ε, $\mu^{(\nu)}$ and $T^{(\nu)}$ are changed simultaneously (when not fixed).

6.2. Ansatz with master equation

The stationary solution of the minimal model was first derived in Ref. [2]. According to the master equation in Eq.(4.13), the dynamics of the state probabilities is described by the following system of differential equations

$$\dot{p}_0 = W_{01}\, p_1 - W_{10}\, p_0 \tag{6.9}$$

$$\dot{p}_1 = W_{10}\, p_0 + W_{12}\, p_2 - (W_{01} + W_{21})\, p_1 \tag{6.10}$$

$$\dot{p}_2 = W_{21}\, p_1 - W_{12}\, p_2. \tag{6.11}$$

It can be written in matrix form as

$$\frac{\mathrm{d}p}{\mathrm{d}t} = \mathbb{W}p = \begin{bmatrix} -W_{10} & W_{01} & 0 \\ W_{10} & -(W_{01}+W_{21}) & W_{12} \\ 0 & W_{21} & -W_{12} \end{bmatrix} p. \tag{6.12}$$

As we are interested in the stationary solution, the most straightforward step is to calculate the null space. The transition probabilities consist of contributions from each reservoir. The rates for the transition $m \to m'$ and its "reverse" $m' \to m$ are related with

$$W_{m'm} = W^{(c)}_{m'm} + W^{(h)}_{m'm} = 1 - W^{(c)}_{mm'} + 1 - W^{(h)}_{mm'} = 2 - W_{mm'}. \tag{6.13}$$

To make the notation more compact, we introduced a normalisation constant Γ and two ratios of transition rates γ_{10} and γ_{21}

$$\gamma_{10} = \frac{W_{01}}{W_{10}} \tag{6.14}$$

$$\gamma_{21} = \frac{W_{12}}{W_{21}} \tag{6.15}$$

$$\Gamma = 1 + \frac{W_{12}}{W_{21}} + \frac{W_{12}W_{01}}{W_{21}W_{10}}. \tag{6.16}$$

With this notation, the stationary solution is found to be

$$p_0^{\mathrm{st}} = \frac{\gamma_{10}\gamma_{21}}{\Gamma} \tag{6.17}$$

$$p_1^{\mathrm{st}} = \frac{\gamma_{21}}{\Gamma} \tag{6.18}$$

$$p_2^{\mathrm{st}} = \frac{1}{\Gamma}, \tag{6.19}$$

which gives rise to the probability fluxes J^c_{10} and J^c_{21}

$$J^{(c)}_{10} = \frac{W^{(c)}_{10}\gamma_{21}}{\Gamma}\left(\gamma_{10} - \left(\frac{1}{W^{(c)}_{10}} - 1\right)\right) \tag{6.20}$$

$$J^{(c)}_{21} = \frac{W^{(c)}_{21}}{\Gamma}\left(\gamma_{21} - \left(\frac{1}{W^{(c)}_{21}} - 1\right)\right) \tag{6.21}$$

With Eq. (5.9), (5.10), (5.24) and (5.25) the particle flux J_N and the energy flux J_E is evaluated to

$$J_N = J^{(c)}_N = \dot{N}^{(c)} = -\dot{N}^{(h)} = J^{(c)}_{10} + J^{(c)}_{21} \tag{6.22}$$

$$J_E = J^{(c)}_E = \dot{E}^{(c)} = -\dot{E}^{(h)} = \varepsilon J^{(c)}_{10} + (\varepsilon + u)J^{(c)}_{21}. \tag{6.23}$$

The full expressions for J_N and J_E can be found in Eq. (A.1) and (A.2) in Sec. A. It's clearly seen that $J_E \not\propto J_N$ breaks the strong coupling condition. Setting $u = 0$ reduces the model to a well-investigated quantum dot, see Ref. [8].

6.3. Regime of the calculation

Finding the point of maximum power and the efficiency at maximum power requires the minimal model to operate as a thermodynamic machine. Heat

needs to be converted into work. However, the minimal model has various 'modus operandi' (heat pump, thermodynamic machine, heater). It's therefore important to know what constraints to the thermodynamic forces $x^{(c)}$ and $x^{(h)}$ are imposed by the condition of working as a thermodynamic machine. To repeat, it is assumed that the temperatures obey

$$T^{(c)} < T^{(h)}. \tag{6.24}$$

So, there is a difference in temperature between the reservoirs and the imagined thermodynamic machine should receive a heat flow from the hot reservoir. All in all, the machine converts heat to chemical work. To do chemical work, the machine needs to transfer particles from a reservoir with low chemical potential to a reservoir with high chemical potential. The temperature difference alone is sufficient to induce a particle flux. Both directions of that particle exchange are possible. However, here it is assumed that the cold reservoir has a lower chemical potential

$$\mu^{(c)} < \mu^{(h)}. \tag{6.25}$$

Thus, particles are transferred from the cold reservoir to the hot reservoir for doing work. The two assumptions constrain the variables $x^{(c)}$ and $x^{(h)}$

$$x^{(c)} > x^{(h)}. \tag{6.26}$$

All possible solutions have to obey Eq. (6.26).

6.4. The point of maximum power

To obtain the efficiency at maximum power, the point of maximum power in the space of $x^{(c)}$ and $x^{(h)}$ needs to be found. The chemical power output of a system in contact with two reservoirs was discussed in Sec. 5.2. Therefore, the power output of the minimal model is given by Eq. (5.34) with the corresponding thermodynamic forces $x^{(c)}$ and $x^{(h)}$ in Eq. (5.31):

$$P = -\dot{W}_{\text{chem}} = T^{(h)}((1-\eta_c)x^{(c)} - x^{(h)})J_N(x^{(c)}, x^{(h)}). \tag{6.27}$$

The power output can now be maximized for a fixed temperature $T^{(h)}$ with regard to $x^{(c)}$ and $x^{(h)}$. This translates to an optimization of the scaled power $P/T^{(h)}$. The derivatives need to be vanishing for the point of maximum power:

$$\frac{\partial P}{\partial x^{(c)}} = T^{(h)}\left[(1-\eta_c)J_N + \left((1-\eta_c)x^{(c)} - x^{(h)}\right)\frac{\partial J}{\partial x^{(c)}}\right] = 0 \tag{6.28}$$

$$\frac{\partial P}{\partial x^{(h)}} = T^{(h)}\left[-J_N + \left((1-\eta_c)x^{(c)} - x^{(h)}\right)\frac{\partial J_N}{\partial x^{(h)}}\right] = 0. \tag{6.29}$$

With Eq. (6.28) and Eq. (6.29), the corresponding variables $x^{(c)}$ and $x^{(h)}$ maximizing the power can be found. After introducing a scaled interaction energy $\hat{u}$ as

$$\hat{u} = \frac{u}{T^{(h)}} \tag{6.30}$$

and substituting $T^{(c)}$ with $T^{(h)}(1-\eta_c)$, these equations solely depend on η_c, $\hat{u}$, $x^{(c)}$ and $x^{(h)}$. Therefore, $x^{(c)}$ and $x^{(h)}$ at the point of maximum power are functions of $\hat{u}$ and η_c. So, for a fixed scaled interaction energy $\hat{u}$ and a fixed Carnot efficiency η_c, values for $x^{(c)}$ and $x^{(h)}$ maximizing power can be found. As the temperature $T^{(h)}$ of the hot reservoir is also fixed in Eq. (6.27), the temperatures of both reservoirs remain constant during the optimisation. Optimizing of the power with regard to $x^{(c)}$ and $x^{(h)}$ equals an optimization with regard to $\varepsilon - \mu^{(c)}$ and $\varepsilon - \mu^{(h)}$ in the non-contracted space. The point of maximum power in the space of $x^{(c)}$ and $x^{(h)}$ is therefore corresponding to an one dimensional manifold in the space of all parameters (ε, $\mu^{(c)}$, $\mu^{(h)}$, $T^{(c)}$ and $T^{(h)}$). Dividing Eq. (6.28) by $(1-\eta_c)$ and adding (6.29) yields

$$\left(x^{(c)} - \frac{x^{(h)}}{1-\eta_c}\right)\left(\frac{\partial J_N}{\partial x^{(c)}} + (1-\eta_c)\frac{\partial J_N}{\partial x^{(h)}}\right) = 0. \tag{6.31}$$

For the product to be zero, one of the factors needs to be zero. One finds for the first bracket

$$x^{(c)} - \frac{x^{(h)}}{1-\eta_c} = 0 \iff \mu^{(c)} = \mu^{(h)}, \tag{6.32}$$

where the chemical potentials of the reservoirs are equal. With even chemical potentials, the power output of the minimal model is zero. Therefore, the first bracket describes a minimum. The optimization condition for maximum power is described by the second bracket

$$\frac{\partial J_N}{\partial x^{(c)}} + (1-\eta_c)\frac{\partial J_N}{\partial x^{(h)}} = 0. \tag{6.33}$$

It can be seen that Eq. (6.33) is also only depending on η_c, $\hat{u}$, $x^{(c)}$ and $x^{(h)}$. For the quantum dot with $\hat{u} = 0$, the equation can be used to get a function $x^{(c)}(x^{(h)})$, see Ref. [8] and Sec. B.2. However, there is no explicit function for a non-vanishing interaction energy. The variables $x^{(c)}$ and $x^{(h)}$ are functions of the Carnot efficiency and can therefore be expanded

$$x^{(c)} = a_0 + a_1\eta_c + a_2\eta_c^2 + \mathcal{O}(\eta_c^3) \tag{6.34}$$
$$x^{(h)} = b_0 + b_1\eta_c + b_2\eta_c^2 + \mathcal{O}(\eta_c^3). \tag{6.35}$$

The coefficients a_i and b_i are depending on $\hat{u}$. Inserting Eq. (6.35) and Eq. (6.35) into the optimization condition and expanding Eq. (6.33) into terms of η_c results in

$$C_0 + C_1\eta_c + C_2\eta_c^2 + \mathcal{O}(\eta_c^3) = 0. \tag{6.36}$$

By comparing coefficients, one sees that the functions C_0, C_1 and C_2 (which are depending on a_i, b_i and $\hat{u}$) each need to be zero for $\eta_c \in [0, 1)$. These conditions can be used to solve for the coefficients a_0, a_1 and a_2. The equation

$C_0(a_0, b_0, \hat{u}) = 0$ has four solutions constraining the coefficient a_0. The first two solutions are given by

$$a_0^{(1)} = b_0 \tag{6.37}$$
$$a_0^{(2)} = -b_0 - \hat{u}. \tag{6.38}$$

The third and fourth solution $a_0^{(3)}$ and $a_0^{(4)}$ can be found in Eq. (B.1) and (B.2) in Sec. B.1. First, one can discard solution $a_0^{(3)}$ and $a_0^{(4)}$ because these solutions do not allow negative interaction energies. The condition in Eq. (B.3) is a lower bound for the interaction energy and requires $\hat{u} > 2$. A general solution should account for positive and negative interaction energies. Also, a solution should reproduce the solution of the quantum dot for no interaction energy $\hat{u} = 0$. For the twofold quantum dot, the coefficients a_0 and b_0 obey $a_0 = b_0$. A derivation is illustrated in the appendix in Sec. B.2. To conclude, the only elligble solution is $a_0^{(1)}$, which will be called a_0 from now.

When comparing coefficients in Eq. (6.36) is continued, $C_1 = 0$ can be used to find one solution for the coefficient a_1. After inserting the solution a_0, a_1 is only depending on b_0 and b_1. But the solution for a_1 is a large expression and is moved to the appendix in Sec. B.3. In the same way, one solution for a_2 can be found by demanding $C_2 = 0$. After elimating a_0 and a_1, the solution for a_2 is a function of b_0, b_1, b_2 and $\hat{u}$. However, the solution for a_2 is a long expression and here

$$a_2(b_0, b_1, b_2, \hat{u}) \tag{6.39}$$

is written instead. Finally, the coefficients a_i of the expansion of $x^{(c)}$ at the point of maximum power are known. The focus is shifted towards determining the coefficients b_0, b_1 and b_2. The missing conditions constraining the coefficients b_i are given by Eq. (6.29). After substituting $x^{(c)}$ and $x^{(h)}$ with the corresponding expansion, the equation can be expanded into terms of the Carnot efficiency η_c, which results in

$$K_0 + K_1\eta_c + K_2\eta_c^2 + K_3\eta_c^3 + \mathcal{O}(\eta_c^4) = 0 \tag{6.40}$$

After eliminating the coefficients a_0, a_1 and a_2 with Eq. (6.37), (B.6) and (6.39), the coefficients K_0 to K_3 are in general depending on b_0, b_1, b_2 and b_3 and a_3:

$$K_0(b_0) + K_1(b_0, b_1)\eta_c + K_2(b_0, b_1, b_2)\eta_c^2 + K_3(b_0, b_1, b_2, a_3, b_3)\eta_c^3 = 0.$$

Here, a_3 and b_3 are the coefficients of the cubic order of an expansion of $x^{(h)}$ and $x^{(h)}$ in η_c, which were not introduced earlier. However, the coefficient K_0 is an identity and is always zero for the solution $a_0 = b_0$. In the same way is K_1 only a function of b_0 and independent from b_1. There is no dependence on the coefficients a_i and b_i with the same order of K_i. So the coefficient K_3 is only depending on b_0, b_1 and b_2 and independent from a_3 and b_3. This is why an extension of the expansion of $x^{(h)}$ and $x^{(h)}$ up to cubic order is not needed

to solve $K_3 = 0$. The same pattern can be recognized, when a quantum dot is investigated, see Ref. [8]. For example, the coefficient K_1 can be found in Eq, (B.7) in Sec. B.4. The resulting expressions for K_2 and K_3 become long and can not be illustrated here in an appropiate manner. As a placeholder for these equations,

$$K_2(b_0, b_1) \tag{6.41}$$
$$K_3(b_0, b_1, b_2) \tag{6.42}$$

is written. Again, comparing coefficients leads to the conditions $K_1 = 0$, $K_2 = 0$ and $K_3 = 0$ because Eq. (6.40) needs to be zero for all $\eta_c \in [0, 1)$. After setting $\hat{u}$ to a fixed interaction energy, Eq. (B.7) can be solved numerically for b_0. Inserting this numerical value for b_0 and the same interaction energy $\hat{u}$ into $K_2 = 0$ leads to a numerical solution for b_1. And finally, with $K_3 = 0$ and b_0, b_1 and the same $\hat{u}$, a solution for b_2 can be obtained. With the coefficients b_0, b_1 and b_2 known for the fixed value of $\hat{u}$, the expansion of $x^{(h)}$ at the point of maximum power up to quadratic order is determined. With Eq. (6.37), (B.6) and (6.39), the expansion of $x^{(c)}$ at the point of maximum power is also characterized. Note that the solutions a_1 and a_2 have poles for specific combinations of $\hat{u}$ and b_0. However, the poles are excluded when the interaction energy is limited to the interval from -0.5 to 0.5. The existence of these poles does not mean that the optimization in general is not working. In fact, it should be seen as something model specific that there is no single point of maximum power (or at least no expansion) for discrete interaction energies. For example, such a pole is found for $\hat{u} = -2$. To rule out issues with branch cuts and other problems, it is continuously checked if the power is actually maximized by the obtained values of $x^{(c)}$ and $x^{(h)}$.

6.5. The efficiency at maximum power

In Eq. (5.35), a general expression for the efficiency is given. For the minimal model, the efficiency takes the form

$$\eta = \frac{x^{(h)} - (1 - \eta_c)x^{(c)}}{x^{(h)} - \hat{u}\frac{f}{g}}, \tag{6.43}$$

where f and g are given by

$$f = \left(\exp\left(x^{(c)}\right) + \exp\left(x^{(h)}\right) + 2\right) \left(\exp\left(\frac{\hat{u}}{(1 - \eta_c)} + x^{(c)}\right) - \exp\left(\hat{u} + x^{(h)}\right)\right) \tag{6.44}$$

$$g = 2\Big[\exp\Big(\frac{\hat{u}}{(1-\eta_c)} + \hat{u} + 2x^{(c)} + x^{(h)}\Big) - \exp\Big(\frac{\hat{u}}{(1-\eta_c)} + \hat{u} + x^{(c)} + 2x^{(h)}\Big) + \exp\Big(\frac{\hat{u}}{(1-\eta_c)} + x^{(c)}\Big) + \exp\Big(\frac{\hat{u}}{(1-\eta_c)} + 2x^{(c)}\Big) - \exp\Big(\hat{u} + x^{(h)}\Big) - \exp\Big(\hat{u} + 2x^{(h)}\Big)\Big]. \quad (6.45)$$

To evaluate the efficiency at maximum power, the expansion of $x^{(c)}$ and $x^{(h)}$ in Eq. (6.35) and (6.35) can be inserted. The coefficients a_0, a_1 and a_2 at the point of maximum power are given by Eq. (6.37), (B.6) and (6.39). Also, numerical values of b_0, b_1 and b_2 were obtained. The efficiency can be expanded into terms of Carnot efficiency after eliminating the coefficients a_0, a_1 and a_2:

$$\eta = c_0 + c_1\eta_c + c_2\eta_c^2 + \mathcal{O}(\eta_c^3). \quad (6.46)$$

The coefficient c_0 is zero. Here, the expression of c_1 is quite large and therefore moved to the appendix, see Eq, (C.1) in Sec. C. It is found that the coefficient c_1 of linear order is only a function of b_0 and can be calculated for different interaction energies $\hat{u}$ and the numerical results for b_0. According to Ref. [24], the linear coefficient has to be bounded upwards by $\frac{1}{2}$ in the linear response regime. It can not easily be seen if the coefficient c_1 has an upper bound of $\frac{1}{2}$. But it becomes apparent, when the numerical results for b_0 are inserted and the linear coefficient is plotted as a function of $\hat{u}$, see Fig. 6.9.

6.6. Numerical results

The numerical solutions of the coefficents a_i and b_i are calculated for interaction energies $|\hat{u}| \leq 0.5$. Small interaction energies are chosen, because the behaviour of the coefficients around $\hat{u} = 0$ is the center of interest. The numerical results for the coefficients a_0 and b_0 are illustrated in Fig. 6.2. It is seen that the

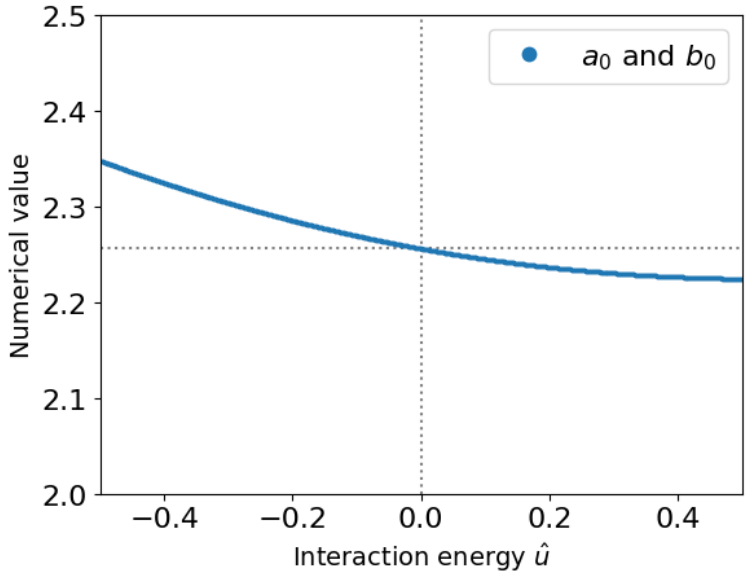

Figure 6.2.: Numerical solution of the coefficients a_0 and b_0 for fixed interaction energies between -0.5 and 0.5. The gray dotted line marks the value of a_0 and b_0 for $\hat{u} = 0$.

coefficients a_0 and b_0 decrease with higher interaction energy. For states near the equilibrium ($\eta_c \ll 1$), where the constant coefficient is dominant, the thermodynamic variables $x^{(c)}$ and $x^{(h)}$ at the point of maximum power, therefore, increase for negative interaction energies and decrease for positive interaction energies in relation to $\hat{u}$.

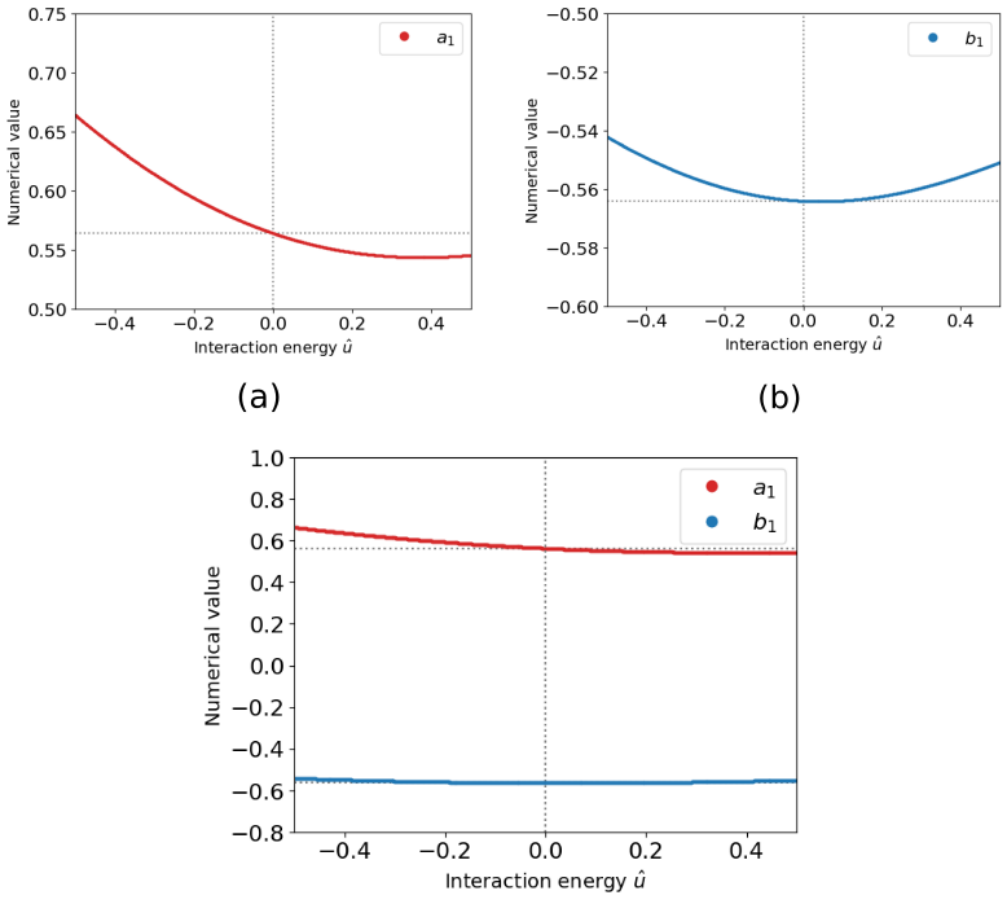

Figure 6.3.: Numerical solution of the coefficient a_1 and b_1 for interaction energies between -0.5 and 0.5. The gray dotted line marks the value of a_1 and b_1 for $\hat{u} = 0$. In (a) a zoomed plot of a_1 is illustrated and in (b) a zoom of b_1 is shown.

In Fig. 6.3, the numerical solutions for the coefficients a_1 and b_1 are shown for interaction energies ranging from -0.5 to 0.5. A general observation is that a_1 is positive and b_1 is negative. This leads to $x^{(c)}$ and $x^{(h)}$ moving away from each other for increasing Carnot efficiencies. The dependency of a_1 and b_1 on the interaction energy $\hat{u}$ controls the magnitude of this splitting. The coefficient a_1 decreases for a positive interaction energies and therefore reduces the splitting of $x^{(c)}$ and $x^{(h)}$. Negative interaction energy would lead to an increase of the splitting. On the other hand, the coefficient b_1 is minimal for $\hat{u} = 0$ and increases for positive and negative interaction energies. In both cases, the splitting of $x^{(c)}$ and $x^{(h)}$ is reduced.

In Fig. 6.4, the numerical results of a_2 and b_2 for small interaction energies $|\hat{u}| \leq 0.5$ are illustrated. Here, a_2 and b_2 show the same behavior for a varying interaction energy. The coefficients are increasing with an increase of $\hat{u}$. Interestingly, the difference of a_2 and b_2 remains almost constant.

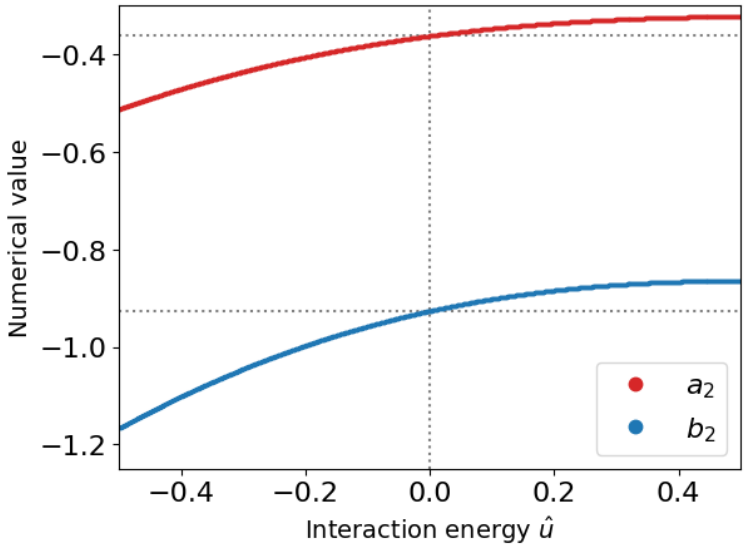

Figure 6.4.: Numerical solution of the coefficients a_2 and b_2 for fixed interaction energies between -0.5 and 0.5. The gray dotted line marks the value of a_2 and b_2 for $\hat{u} = 0$

The expansion of $x^{(c)}$ and $x^{(h)}$ in Carnot efficiency is illustrated in Fig. 6.5 and Fig. 6.6. It can be seen that the interaction energy $\hat{u}$ does not really change the general behavior of $x^{(c)}$ and $x^{(h)}$. The monotone increase of $x^{(c)}$ and the monotone decrease of $x^{(h)}$ is nearly independent of $\hat{u}$. For an increasing Carnot efficiency, the variables $x^{(c)}$ and $x^{(h)}$ move away from each other. That is equivalent to a higher gradient of the chemical potentials and is also observed in the quantum dot, see Ref. [8]. For a greater temperature difference (bigger Carnot efficiency), the capacity to do work is raised and the gradient of the chemical potentials can be higher. It can be seen that $x^{(c)} = x^{(h)}$ holds for small Carnot efficiencies $\eta_c \to 0$. Therefore, when the difference in temperature is small, the gradient of the chemical potentials is also low. This is why the minimal model at maximum power is in the linear response regime. However, there is an impact of the interaction energy $\hat{u}$ that shifts the values of $x^{(c)}$ and $x^{(h)}$ downwards and the strength of the shift is declining with rising interaction energy. When $\hat{u}$ increases, the values of $x^{(c)}$ and $x^{(h)}$ are lowered for a fixed Carnot efficiency and the point of maximum power is moved towards lower $x^{(c)}$ and $x^{(h)}$. Thus, the point of maximum power is also moved towards higher chemical potentials $\mu^{(c)}$ and $\mu^{(h)}$. After plotting the difference $x^{(c)} - x^{(h)}$ (not done here), it can be seen that both terms approach each other for increasing interaction energy.

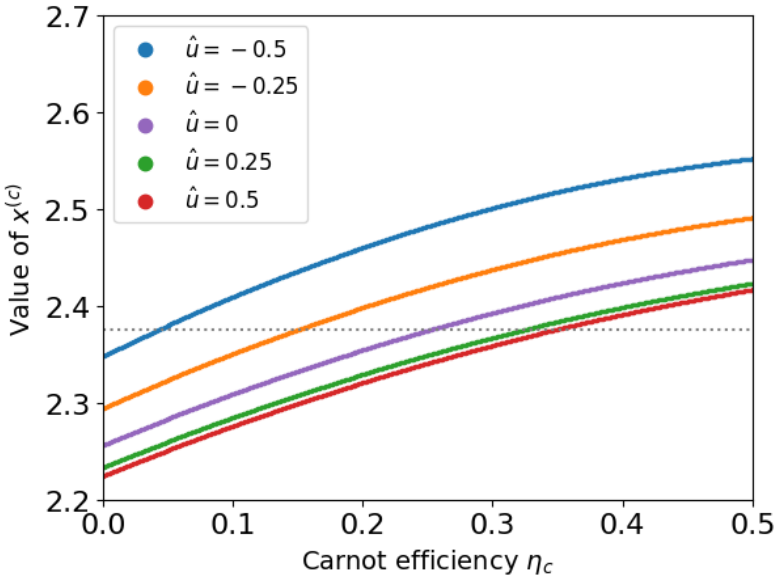

Figure 6.5.: Expansion of $x^{(c)}$ up to quadratic order for interaction energies -0.5, -0.25, 0, 0.25 and 0.5. The gray dotted line shows how a change of the interaction energy can be compensated by varying η_c.

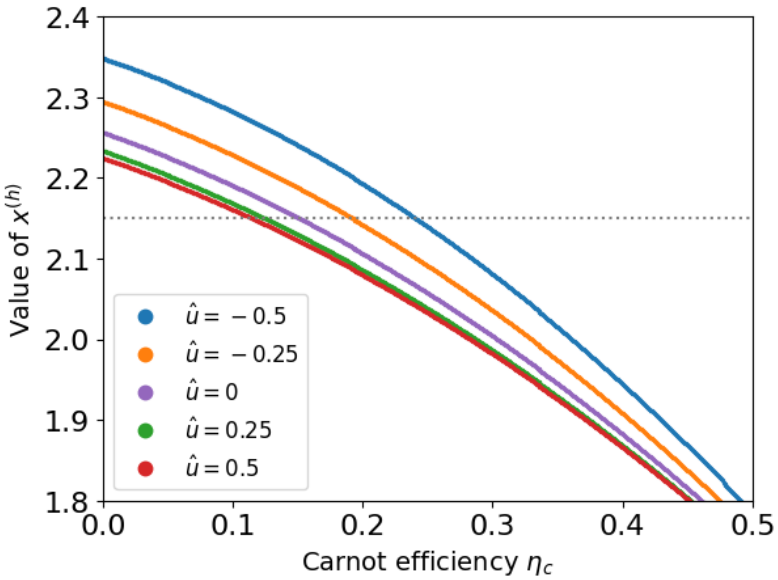

Figure 6.6.: Expansion of $x^{(h)}$ up to quadratic order for interaction energies -0.5, -0.25, 0, 0.25 and 0.5. The gray dotted line shows how a change of the interaction energy can be compensated by varying η_c.

This means also that the chemical potentials are brought closer together. For $\hat{u} \to \infty$, state 2 is blocked and the minimal model becomes a quantum dot with two states, see Ref. [8]. So, $x^{(c)}$ and $x^{(h)}$ are bounded downwards by the corresponding $x^{(c)}$ and $x^{(h)}$ of the quantum dot. When one wants to extract the maximum power out of the minimal model, it is wise to bring the chemical potentials $\mu^{(c)}$ and $\mu^{(h)}$ closer to the energy ε and to each other for an increasing $\hat{u}$. It is also seen in Fig. 6.5 and Fig. 6.6, that an increase of the interaction energy $\hat{u}$ can be compensated by an increase of the Carnot efficiency, see Fig. D.1 in Sec. D. In the end, positive interaction energy moves the point of maximum power towards equilibrium and impedes the power extraction in the sense that it blocks off higher chemical gradients from the maximum power regime. In contrast, negative interaction energy moves the point of maximum power away from equilibrium and requires a higher gradient of the chemical potentials to extract maximum power.

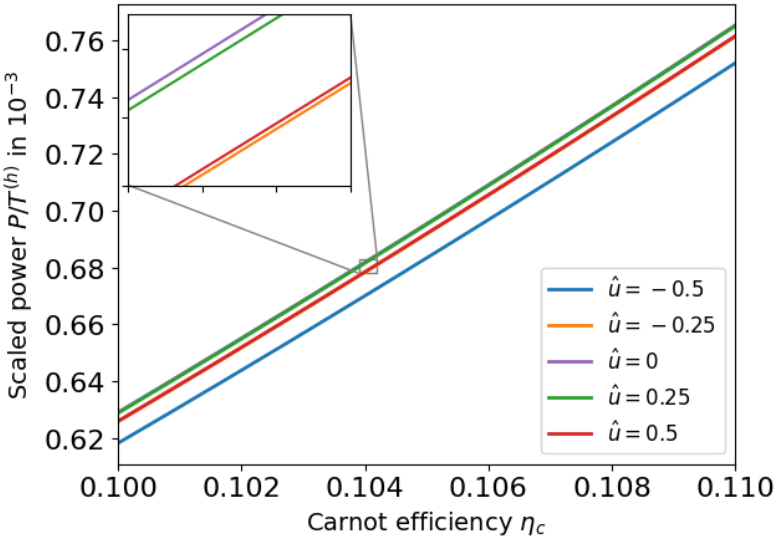

Figure 6.7.: The scaled power $\frac{P}{T^{(h)}}$ is illustrated in dependence of the Carnot efficiency η_c for the interaction energies -0.5, -0.25, 0, 0.25 and 0.5 at the point of maximum power. Only a small interval of η_c is shown. A part of the plot is also zoomed in to show that the plots for $\hat{u} = 0$ and $\hat{u} = 0.25$ as well as the plots for $\hat{u} = -0.25$ and $\hat{u} = 0.5$ are very close together.

In Fig. 6.7, the optimized scaled power $\frac{P}{T^{(h)}}$ is shown for the interaction energies -0.5, -0.25, 0, 0.25 and 0.5 in dependence of the Carnot efficiency. It is seen that the maximum power is the highest for an interaction energy of $\hat{u} = 0$. Negative interaction energy lowers the power output at the point of maximum power the most. Positive interaction energy also decreases the maximum power output. To summarize, non-zero interaction energy lowers the maximum power output.

In Fig. 6.8, the efficiency of the minimal model at maximum power is illustrated in comparison to the Carnot efficiency and the Curzon-Ahlborn efficiency for the interaction energies -0.5, 0 and 0.5. It is seen that a positive interaction energy $\hat{u}$ increases the efficiency. In that case, the efficiency is higher than the Curzon.Ahlborn efficiency. On the other hand, a negative $\hat{u}$ lowers the efficiency. While the maximum power is reduced for positive interaction energy, it provides the benefit that the minimal model works with higher efficiency. A negative $\hat{u}$ seems to have only downsides, e.g. a reduced efficiency and maximum power.

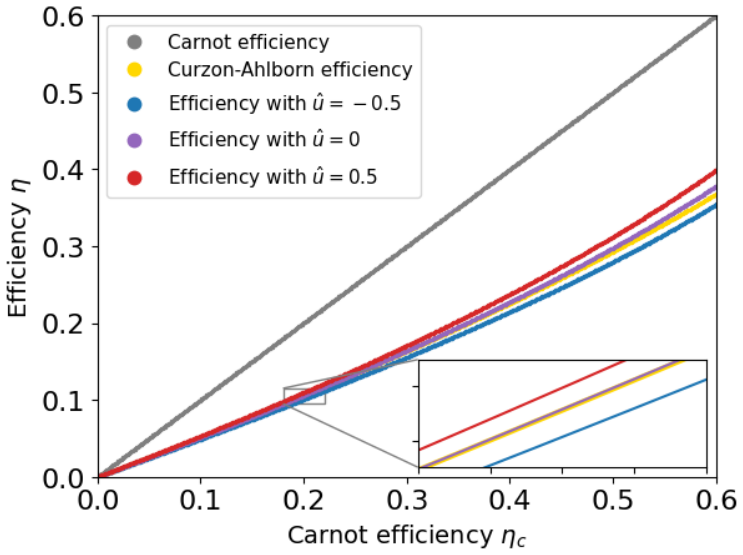

Figure 6.8.: Efficiency of the minimal model at maximum power for small Carnot efficiencies from 0 to 0.6. The interaction energy is set to -0.5, 0 and 0.5. The Curzon-Ahlborn efficiency and the Carnot efficiency are also shown.

Finally, the focus can be shifted to the expansion of the efficiency into terms of Carnot efficiency. The linear coefficient is shown in Eq. (C.1). According to Ref. [24], there is an upper bound of $\frac{1}{2}$ in the regime of linear response. In Fig. 6.9, the linear coefficient is illustrated as a function of $\hat{u}$. The values of b_0 were calculated numerically for different interaction energies. Then, the linear coefficient can be plotted as a function of the interaction energy $\hat{u}$. For positive interaction energies, it is seen that the linear coefficient reaches values over $\frac{1}{2}$, which is the supposed upper bound. For negative $\hat{u}$, the linear coefficient is less than $\frac{1}{2}$.

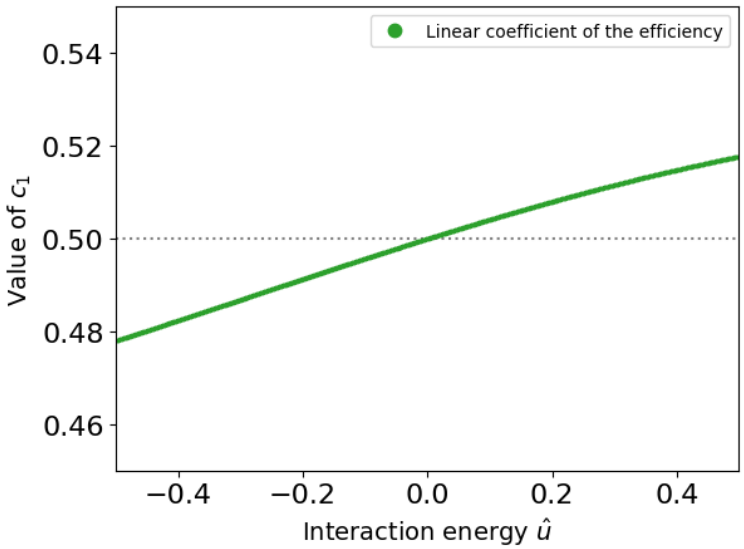

Figure 6.9.: The efficiency is expanded into terms of Carnot efficiency and only the linear coefficient c_1 in Eq. (6.46) is shown for small $\hat{u}$ ranging from -0.5 to 0.5. The gray dotted line stands for the upper bound of $\frac{1}{2}$. The expression for c_1 can be found in Eq. (C.1).

7. Conclusion

In this work, foundations for macroscopic thermodynamics and stochastic thermodynamics were presented. The Carnot efficiency and the Curzon-Ahlborn efficiency were derived to understand the requirements and the boundaries. Then, the focus was shifted to the minimal model as a realistic system incorporating particle interaction. The optimization of the minimal model with regard to power revealed that the interaction energy has an impact on various aspects. First, the point of maximum power is either moved closer to equilibrium or moved away from equilibrium. Further, negative interaction energy leads to a smaller maximum power and to less efficiency at maximum power. In contrast, repulsion has a positive influence on the efficiency, as the minimal model with repulsion is more efficient than the quantum dot ($\hat{u} = 0$). The amount of maximum power is still reduced in comparison to the quantum dot, but not as much as for a negative $\hat{u}$. Others have reported a significant decrease of efficiency, when strong coupling is broken, see Ref. [17]. All in all, the presence of interaction in a microscopic thermodynamic machine has not necessarily a negative impact. For the cost of a small decrease of maximum power, the efficiency can be raised for positive interaction energies. As the minimal model turns into a regular quantum dot for $\hat{u} \to \infty$ and into a twofold quantum dot for $\hat{u} = 0$ (both show the same efficiency at maximum power), there has to be a specific positive interaction energy, which corresponds to the highest efficiency at the point of maximum power. In other words, the minimal model can be tuned with regard to the interaction energy to extract maximum power with the highest efficiency. It is interesting if this interaction energy has any deeper meaning. The numerical calculation of the mentioned interaction energy can be done by extending the numerical calculations to larger interaction energies. Surprisingly, the linear coefficient of an expansion of the efficiency breaks the upper bound of $\frac{1}{2}$. The upper bound was proven for thermodynamic systems at maximum power in the linear response regime, see Ref. [24]. However, the minimal model is for small Carnot efficiencies definitely in the regime of linear response. The fact that the minimal model at maximum power breaks the upper boundary for the linear coefficient could mean that there are inconsistencies between stochastic thermodynamics and linear irreversible thermodynamics regarding the efficiency at maximum power.

Bibliography

[1] A. E. Allahverdyan, R. S. Johal, and G. Mahler. Work extremum principle: Structure and function of quantum heat engines. *Physical Review E*, 77(4):041118, Apr. 2008.

[2] A. Barth. Entropieproduktion und Onsagerkoeffizienten in Nichtgleichgewichtszuständen eines Hopping-Modells [Entropy production and onsager coefficients in non-equilibrium states of a hopping model]. Bachelor's thesis, University Osnabrück, Dec. 2019.

[3] C. Bustamante, J. Liphardt, and F. Ritort. The Nonequilibrium Thermodynamics of Small Systems. *Physics Today*, 58(7):43–48, July 2005.

[4] S. Carnot. Réflexions sur la puissance motrice du feu et sur les machines propres à développer cette puissance [Reflections on the motive power of fire and on the machines suitable for developing this power]. *Annales scientifiques de l'École Normale Supérieure*, 2(1):393–457, 1872.

[5] R. Clausius. Über die bewegende Kraft der Wärme und die Gesetze, welche sich daraus für die Wärmelehre selbst ableiten lassen [The moving force of heat and the laws which can be derived therefrom for heat theory itself]. *Annalen der Physik*, 155(3):368–397, 1850.

[6] R. Clausius. Über verschiedene für die Anwendung bequeme Formen der Hauptgleichungen der mechanischen Wärmetheorie [On various forms of the main equations of the mechanical theory of heat, convenient for application]. *Annalen der Physik*, 201(7):353–400, 1865.

[7] F. L. Curzon and B. Ahlborn. Efficiency of a Carnot engine at maximum power output. *American Journal of Physics*, 43(1):22–24, Jan. 1975.

[8] M. Esposito, K. Lindenberg, and C. V. den Broeck. Thermoelectric efficiency at maximum power in a quantum dot. *EPL (Europhysics Letters)*, 85(6):60010, mar 2009.

[9] M. Esposito, K. Lindenberg, and C. Van den Broeck. Universality of efficiency at maximum power. *Phys. Rev. Lett.*, 102:130602, Apr 2009.

[10] R. J. Glauber. Time-Dependent Statistics of the Ising Model. *Journal of Mathematical Physics*, 4(2):294–307, Feb. 1963.

[11] A. Gomez-Marin and J. M. Sancho. Tight coupling in thermal Brownian motors. *Physical Review E*, 74(6):062102, Dec. 2006.

[12] Y. Izumida and K. Okuda. Molecular kinetic analysis of a finite-time Carnot cycle. *EPL (Europhysics Letters)*, 83(6):60003, Sept. 2008.

[13] P. Maaß. Lecture notes: Introduction to thermodynamics. unpublished, Jan. 2021.

[14] D. J. Müller and Y. F. Dufrêne. Atomic force microscopy as a multifunctional molecular toolbox in nanobiotechnology. *Nature Nanotechnology*, 3(5):261–269, May 2008.

[15] L. Onsager. Reciprocal relations in irreversible processes. i. *Phys. Rev.*, 37:405–426, Feb 1931.

[16] M. Peltier. Nouvelles expériences sur la caloricité des courants électrique [New experiments on the heat effects of electric currents]. *Annales de Chimie et de Physique*, 56:371–386, 1834.

[17] B. Rutten, M. Esposito, and B. Cleuren. Reaching optimal efficiencies using nanosized photoelectric devices. *Phys. Rev. B*, 80:235122, Dec 2009.

[18] T. Schmiedl and U. Seifert. Efficiency at maximum power: An analytically solvable model for stochastic heat engines. *EPL (Europhysics Letters)*, 81(2):20003, Dec. 2007.

[19] J. Schnakenberg. Network theory of microscopic and macroscopic behavior of master equation systems. *Rev. Mod. Phys.*, 48:571–585, Oct 1976.

[20] H. E. D. Scovil and E. O. Schulz-DuBois. Three-Level Masers as Heat Engines. *Physical Review Letters*, 2(6):262–263, Mar. 1959.

[21] T. J. Seebeck. Magnetische Polarisation der Metalle und Erze durch Temperaturdifferenz [Magnetic polarization of metals and ores by temperature differences]. *Abhandlungen der Königlichen Akademie der Wissenschaften zu Berlin*, page 265–373, 1822.

[22] C. E. Shannon. A mathematical theory of communication. *The Bell System Technical Journal*, 27(3):379–423, 1948.

[23] W. Thomson. On the dynamical theory of heat, with numerical results deduced from mr joule's equivalent of a thermal unit, and m. regnault's observations on steam. *Transactions of the Royal Society of Edinburgh*, 20(2):261–268, 1851.

[24] C. Van den Broeck. Thermodynamic efficiency at maximum power. *Phys. Rev. Lett.*, 95:190602, Nov 2005.

[25] C. Van den Broeck. Stochastic thermodynamics: A brief introduction. *Proc. Of the International School of Physics 'Enrico Fermi'*, 184, 09 2014.

[26] N. G. van Kampen. *Stochastic Processes in Physics and Chemistry*. Elsevier, Amsterdam, 2007.

A. Full expressions of the particle and energy flux

The energy and particle flux of the minimal model are introduced in Sec. 6.2. The particle flux J_N and the energy flux J_E take the form

$$J_N = 2B\Bigg[\frac{\left(\exp\left(\frac{u}{T^{(c)}}+x^{(c)}\right)+1\right)^{-1}-1}{\exp\left(x^{(h)}\right)+1} - \frac{1}{\left(\exp\left(x^{(c)}\right)+1\right)\left(\exp\left(\frac{u}{T^{(h)}}+x^{(h)}\right)+1\right)} + \frac{1}{\exp\left(x^{(c)}\right)+1}\Bigg] \tag{A.1}$$

$$\begin{aligned} J_E = 2B\epsilon\Bigg[&\frac{\left(\exp\left(\frac{u}{T^{(c)}}+x^{(c)}\right)+1\right)^{-1}-1}{\exp\left(x^{(h)}\right)+1} \\ &- \frac{1}{\left(\exp\left(x^{(c)}\right)+1\right)\left(\exp\left(\frac{u}{T^{(h)}}+x^{(h)}\right)+1\right)} + \frac{1}{\exp\left(x^{(c)}\right)+1}\Bigg] \\ &+ u\left[\frac{1}{\exp\left(x^{(c)}\right)+1}+\frac{1}{\exp\left(x^{(h)}\right)+1}\right] \\ &\left[\frac{1}{\exp\left(\frac{u}{T^{(c)}}+x^{(c)}\right)+1}-\frac{1}{\exp\left(\frac{u}{T^{(h)}}+x^{(h)}\right)+1}\right] \end{aligned} \tag{A.2}$$

with B being

$$B = \left[\frac{\frac{1}{\exp\left(x^{(c)}\right)+1}+\frac{1}{\exp\left(x^{(h)}\right)+1}-2}{\exp\left(\frac{u}{T^{(c)}}+x^{(c)}\right)+1} + \frac{\frac{1}{\exp\left(x^{(c)}\right)+1}+\frac{1}{\exp\left(x^{(h)}\right)+1}-2}{\exp\left(\frac{u}{T^{(h)}}+x^{(h)}\right)+1} + 4\right]^{-1}.$$

B. Supplement to the point of maximum power

B.1. The solutions $a_0^{(3)}$ and $a_0^{(4)}$

In Sec. 6.4, solving $C_0(a_0, b_0, \hat{u}) = 0$ leads to four solutions of a_0. The third and fourth solution are given by

$$a_0^{(3)} = \log\Bigg(\frac{1}{8e^{b_0+\hat{u}} + 4e^{2b_0+2\hat{u}} + e^{\hat{u}} + 2} \Bigg[-9e^{b_0+\hat{u}} - 4e^{2b_0+\hat{u}} + 2e^{b_0+2\hat{u}} - 2e^{b_0} - 4 - 2e^{\hat{u}}\sqrt{R_1} - 16e^{b_0+\hat{u}}\sqrt{R_2} - 4\sqrt{R_3} - 8e^{2b_0+2\hat{u}}\sqrt{R_4}\Bigg]\Bigg) \quad \text{(B.1)}$$

$$a_0^{(4)} = \log\Bigg(\frac{1}{8e^{b_0+\hat{u}} + 4e^{2b_0+2\hat{u}} + e^{\hat{u}} + 2} \Bigg[-9e^{b_0+\hat{u}} - 4e^{2b_0+\hat{u}} + 2e^{b_0+2\hat{u}} - 2e^{b_0} - 4 - 2e^{\hat{u}}\sqrt{R_1} - 16e^{b_0+\hat{u}}\sqrt{R_2} - 4\sqrt{R_3} + 8e^{2b_0+2\hat{u}}\sqrt{R_4}\Bigg]\Bigg) \quad \text{(B.2)}$$

with

$$R_1 = \frac{8e^{b_0+\hat{u}} - 4e^{b_0+2\hat{u}} + 14e^{2b_0+2\hat{u}} + 8e^{3b_0+2\hat{u}} + 2e^{4b_0+2\hat{u}}}{\left(8e^{b_0+\hat{u}} + 4e^{2b_0+2\hat{u}} + e^{\hat{u}} + 2\right)^2} + \frac{-9e^{2b_0+3\hat{u}} - 4e^{3b_0+3\hat{u}} - e^{4b_0+3\hat{u}} + e^{2b_0+4\hat{u}} - e^{\hat{u}} + 2}{\left(8e^{b_0+\hat{u}} + 4e^{2b_0+2\hat{u}} + e^{\hat{u}} + 2\right)^2}$$

$$R_2 = \frac{8e^{b_0+\hat{u}} - 4e^{b_0+2\hat{u}} + 14e^{2b_0+2\hat{u}} + 8e^{3b_0+2\hat{u}} + 2e^{4b_0+2\hat{u}}}{\left(8e^{b_0+\hat{u}} + 4e^{2b_0+2\hat{u}} + e^{\hat{u}} + 2\right)^2} + \frac{-9e^{2b_0+3\hat{u}} - 4e^{3b_0+3\hat{u}} - e^{4b_0+3\hat{u}} + e^{2b_0+4\hat{u}} - e^{\hat{u}} + 2}{\left(8e^{b_0+\hat{u}} + 4e^{2b_0+2\hat{u}} + e^{\hat{u}} + 2\right)^2}$$

$$R_3 = \frac{8e^{b_0+\hat{u}} - 4e^{b_0+2\hat{u}} + 14e^{2b_0+2\hat{u}} + 8e^{3b_0+2\hat{u}} + 2e^{4b_0+2\hat{u}} - 9e^{2b_0+3\hat{u}}}{\left(8e^{b_0+\hat{u}} + 4e^{2b_0+2\hat{u}} + e^{\hat{u}} + 2\right)^2} + \frac{-4e^{3b_0+3\hat{u}} - e^{4b_0+3\hat{u}} + e^{2b_0+4\hat{u}} - e^{\hat{u}} + 2}{\left(8e^{b_0+\hat{u}} + 4e^{2b_0+2\hat{u}} + e^{\hat{u}} + 2\right)^2}$$

$$R_4 = \frac{8e^{b_0+\hat{u}} - 4e^{b_0+2\hat{u}} + 14e^{2b_0+2\hat{u}} + 8e^{3b_0+2\hat{u}} + 2e^{4b_0+2\hat{u}} - 9e^{2b_0+3\hat{u}}}{\left(8e^{b_0+\hat{u}} + 4e^{2b_0+2\hat{u}} + e^{\hat{u}} + 2\right)^2} \frac{-4e^{3b_0+3\hat{u}} - e^{4b_0+3\hat{u}} + e^{2b_0+4\hat{u}} - e^{\hat{u}} + 2}{\left(8e^{b_0+\hat{u}} + 4e^{2b_0+2\hat{u}} + e^{\hat{u}} + 2\right)^2}$$

and the condition

$$\hat{u} > \log\Bigg(\frac{e^{-2b_0}\sqrt[3]{\sqrt{A}+B}}{3\sqrt[3]{2}} + \frac{1}{3}\left(4e^{b_0} + e^{2b_0} + 7\right) - \frac{\sqrt[3]{2}e^{-2b_0}\left(-e^{4b_0}\left(4e^{b_0} + e^{2b_0} + 7\right)^2 - 12e^{3b_0}\right)}{3\sqrt[3]{\sqrt{C}+D}}\Bigg), \quad \text{(B.3)}$$

where A, B, C and D are given by

$$A = 729e^{8b_0} + 6696e^{9b_0} + 23652e^{10b_0} + 41256e^{11b_0} + 39204e^{12b_0} + 21600e^{13b_0} + 7020e^{14b_0} + 1296e^{15b_0} + 108e^{16b_0}$$

$$B = 27e^{4b_0} + 252e^{5b_0} + 830e^{6b_0} + 1212e^{7b_0} + 966e^{8b_0} + 464e^{9b_0} + 138e^{10b_0} + 24e^{11b_0} + 2e^{12b_0}$$

$$C = 729e^{8b_0} + 6696e^{9b_0} + 23652e^{10b_0} + 41256e^{11b_0} + 39204e^{12b_0} + 21600e^{13b_0} + 7020e^{14b_0} + 1296e^{15b_0} + 108e^{16b_0}$$

$$D = 27e^{4b_0} + 252e^{5b_0} + 830e^{6b_0} + 1212e^{7b_0} + 966e^{8b_0} + 464e^{9b_0} + 138e^{10b_0} + 24e^{11b_0} + 2e^{12b_0}.$$

B.2. Efficiency of the twofold quantum dot at maximum power

When there is no interaction energy present in the minimal model, it is a twofold quantum dot. The expression of the power in Eq. (5.34) is still valid. This leads to the optimization conditions in Eq. (6.28) and Eq. (6.29) with $\hat{u} = 0$. Dividing Eq. (6.28) by $(1-\eta_c)$ and adding Eq. (6.29) leads to the same combined optimization condition in Eq. (6.33). For $\hat{u} = 0$, the equation can be solved for $x^{(c)}$ as a function of $x^{(h)}$

$$x^{(c)}(x^{(h)}). \tag{B.4}$$

The expression is large and can not be illustrated here. An expansion of $x^{(c)}$ into terms of Carnot efficiency can be acquired by inserting the expansion of $x^{(h)}$ in Eq.(6.35) into the solution in Eq. (B.4). The resulting expression can be expanded in terms of Carnot efficiency

$$x^{(c)} = a_0 + a_1\eta_c + a_2\eta_c^2 = b_0 + a_1(b_0, b_1)\eta_c + a_2(b_0, b_1, b_2)\eta_c^2, \tag{B.5}$$

where it can be immediately seen that a_0 equals b_0.

B.3. The solution for a_1

In Sec. 6.4, it is mentioned how to obtain a solution for the coefficient a_1. The solution has the form

$$\begin{aligned} a_1 = \frac{\left(e^{b_0}+1\right)^2 e^{-b_0-\hat{u}}\left(e^{b_0+\hat{u}}+1\right)^2\left(e^{b_0+\hat{u}}+e^{2b_0+\hat{u}}+1\right)^2}{C} \cdot \\ \left(\frac{b_1 e^{b_0+\hat{u}} A}{2\left(e^{b_0}+1\right)^2\left(e^{b_0+\hat{u}}+1\right)^2\left(e^{b_0+\hat{u}}+e^{2b_0+\hat{u}}+1\right)^2}\right. \\ \left. + \frac{e^{b_0+\hat{u}} B}{2\left(e^{b_0}+1\right)\left(e^{b_0+\hat{u}}+1\right)^2\left(e^{b_0+\hat{u}}+e^{2b_0+\hat{u}}+1\right)^2}\right), \end{aligned} \tag{B.6}$$

where the functions A, B and C are given by

$$\begin{aligned} A = e^{2(b_0+\hat{u})} - 4e^{2b_0+\hat{u}} + 2e^{4b_0+\hat{u}} + 4e^{4b_0+2\hat{u}} \\ + 4e^{5b_0+2\hat{u}} - e^{4b_0+3\hat{u}} + e^{6b_0+3\hat{u}} - 4e^{b_0} - 2e^{2b_0} - 1 \end{aligned}$$

$$\begin{aligned} B = -(\hat{u}-6)e^{2b_0+\hat{u}} + 2e^{b_0+\hat{u}} + e^{4b_0+3\hat{u}} \\ + e^{5b_0+3\hat{u}} - (\hat{u}-2)e^{3b_0+\hat{u}} - (\hat{u}-1)e^{2(b_0+\hat{u})} + e^{b_0}(\hat{u}+2) \\ + (3-2\hat{u})e^{4b_0+2\hat{u}} + (5-3\hat{u})e^{3b_0+2\hat{u}} + \hat{u} + 1 \end{aligned}$$

$$\begin{aligned} C = e^{2(b_0+\hat{u})} - 4e^{2b_0+\hat{u}} + 2e^{4b_0+\hat{u}} + 4e^{4b_0+2\hat{u}} \\ + 4e^{5b_0+2\hat{u}} - e^{4b_0+3\hat{u}} + e^{6b_0+3\hat{u}} - 4e^{b_0} - 2e^{2b_0} - 1. \end{aligned}$$

B.4. Linear order of the second optimization condition

In Sec. 6.4, the second optimization condition in Eq. (6.29) is expanded into terms of Carnot efficiency. The linear coefficient K_1 takes the form

$$K_1 = \frac{e^{b_0+\hat{u}}\left(-b_0 A + \left(e^{b_0}+1\right)B\right)}{2\left(e^{b_0}+1\right)\left(e^{b_0+\hat{u}}+1\right)\left(e^{b_0+\hat{u}}+e^{2b_0+\hat{u}}+1\right)C}, \tag{B.7}$$

where A, B and C are given by

$$\begin{aligned} A = {} & e^{2(b_0+\hat{u})} - 5e^{2b_0+\hat{u}} - 12e^{3b_0+\hat{u}} + 4e^{5b_0+\hat{u}} + 2e^{3b_0+2\hat{u}} \\ & + 12e^{5b_0+2\hat{u}} + 10e^{6b_0+2\hat{u}} - 2e^{5b_0+3\hat{u}} + 5e^{6b_0+3\hat{u}} + 6e^{7b_0+3\hat{u}} \\ & - e^{6b_0+4\hat{u}} + e^{8b_0+4\hat{u}} - 6e^{b_0} - 10e^{2b_0} - 4e^{3b_0} - 1 \end{aligned}$$

$$\begin{aligned} B = {} & -4(\hat{u}-8)e^{3b_0+\hat{u}} + 4e^{b_0+\hat{u}} + 2e^{6b_0+4\hat{u}} + 2e^{7b_0+4\hat{u}} \\ & - 2(\hat{u}-4)e^{4b_0+\hat{u}} - (\hat{u}-2)e^{2(b_0+\hat{u})} + 2e^{b_0}(\hat{u}+4) \\ & + 2e^{2b_0}(\hat{u}+4) - 2(5\hat{u}-9)e^{3b_0+2\hat{u}} + (4-3\hat{u})e^{4b_0+3\hat{u}} \\ & + (10-3\hat{u})e^{6b_0+3\hat{u}} + (22-4\hat{u})e^{2b_0+\hat{u}} + (16-6\hat{u})e^{5b_0+2\hat{u}} \\ & + (16-6\hat{u})e^{5b_0+3\hat{u}} + (38-14\hat{u})e^{4b_0+2\hat{u}} + \hat{u} + 2 \end{aligned}$$

$$\begin{aligned} C = {} & e^{2(b_0+\hat{u})} - 4e^{2b_0+\hat{u}} + 2e^{4b_0+\hat{u}} + 4e^{4b_0+2\hat{u}} \\ & + 4e^{5b_0+2\hat{u}} - e^{4b_0+3\hat{u}} + e^{6b_0+3\hat{u}} - 4e^{b_0} - 2e^{2b_0} - 1. \end{aligned}$$

C. The linear coefficient c_1 of the efficiency

In Sec. 6.5, the efficiency is expanded into terms of Carnot efficiency. The linear coefficient c_1 is only a function of b_0 and $\hat{u}$. It takes the form

$$c_1 = \frac{b_0 - \left(e^{b_0} + 1\right) \frac{A}{B}}{b_0 - \frac{C}{D}\hat{u}} \tag{C.1}$$

with A, B, C and D being

$$\begin{aligned} A = (\hat{u} - 6)\left(-e^{2b_0+\hat{u}}\right) + 2e^{b_0+\hat{u}} + e^{4b_0+3\hat{u}} + e^{5b_0+3\hat{u}} \\ - (\hat{u} - 2)e^{3b_0+\hat{u}} - (\hat{u} - 1)e^{2(b_0+\hat{u})} + e^{b_0}(\hat{u} + 2) \\ + (3 - 2\hat{u})e^{4b_0+2\hat{u}} + (5 - 3\hat{u})e^{3b_0+2\hat{u}} + \hat{u} + 1 \end{aligned}$$

$$\begin{aligned} B = e^{2(b_0+\hat{u})} - 4e^{2b_0+\hat{u}} + 2e^{4b_0+\hat{u}} + 4e^{4b_0+2\hat{u}} + 4e^{5b_0+2\hat{u}} \\ - e^{4b_0+3\hat{u}} + e^{6b_0+3\hat{u}} - 4e^{b_0} - 2e^{2b_0} - 1 \end{aligned}$$

$$\begin{aligned} C = -2e^{b_0}\hat{u} - e^{2b_0}\hat{u} - 3\hat{u}e^{2b_0+\hat{u}} - \hat{u}e^{3b_0+\hat{u}} + \hat{u}e^{4b_0+\hat{u}} - \hat{u}e^{3b_0+2\hat{u}} \\ + \hat{u}e^{5b_0+2\hat{u}} + e^{b_0+\hat{u}} + 5e^{2b_0+\hat{u}} + 6e^{3b_0+\hat{u}} + 2e^{4b_0+\hat{u}} \\ + e^{3b_0+2\hat{u}} + 2e^{4b_0+2\hat{u}} + e^{5b_0+2\hat{u}} + 3e^{b_0} + 2e^{2b_0} + 1 \end{aligned}$$

$$\begin{aligned} D = \left(e^{b_0+\hat{u}} + e^{2b_0+\hat{u}} + 1\right)(-e^{b_0}\hat{u} - 2\hat{u}e^{2b_0+\hat{u}} - \hat{u}e^{3b_0+\hat{u}} \\ + 2e^{2b_0+\hat{u}} + 4e^{3b_0+\hat{u}} + e^{4b_0+2\hat{u}} + 4e^{b_0} + 4e^{2b_0} + 1). \end{aligned}$$

D. Plots of the thermodynamic variables

In Sec. 6.6, it was mentioned that an increasing interaction energy $\hat{u}$ can be compensated by increasing the Carnot efficiency η_c to achieve maximum power. This is illustrated in Fig. D.1, where the Carnot efficiency is shown in dependence of values of $x^{(c)}$ and $x^{(h)}$ for interaction energies -0.5, -0.25, 0, 0.25 and 0.5. For fixed values of $x^{(c)}$ and $x^{(h)}$, different combinations of the Carnot efficiency η_c and the interaction energy $\hat{u}$ achieve maximum power. For example, the combinations can be found in Fig. D.1 by looking at the intersections with the gray dotted line.

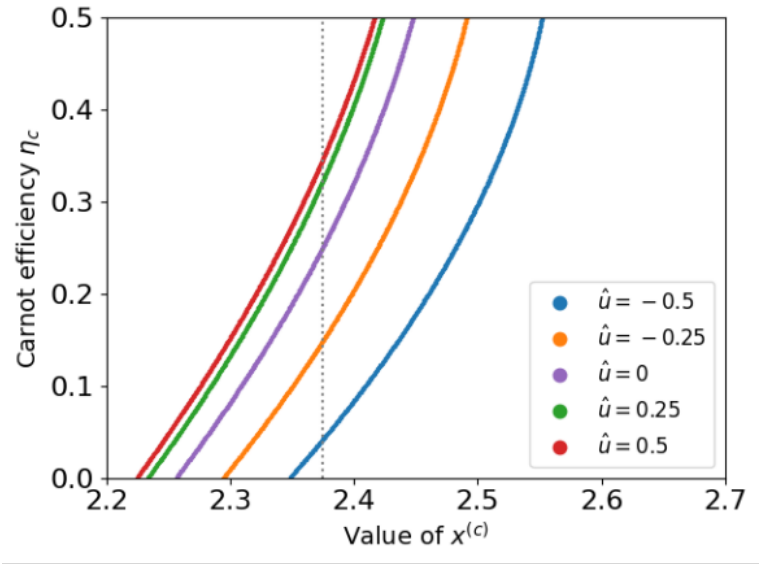

(a)

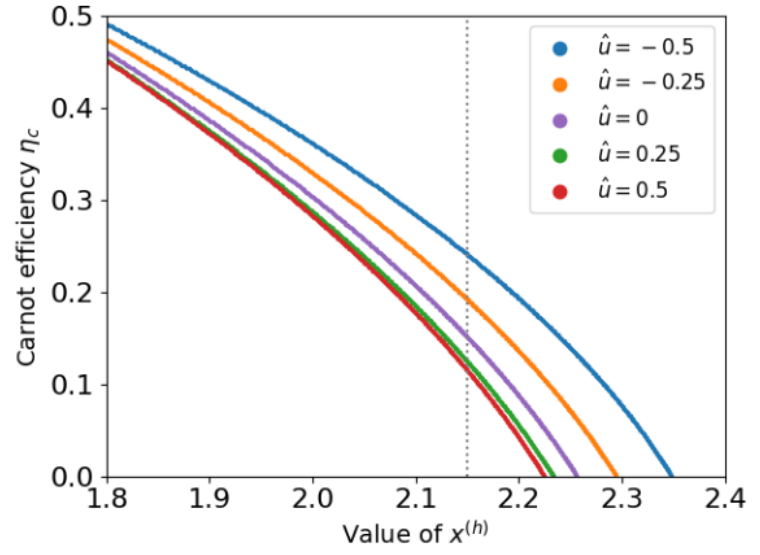

(b)

Figure D.1.: The Carnot efficiency is illustrated in dependence of $x^{(c)}$ (a) and $x^{(c)}$ (b) and for interaction energies -0.5, -0.25, 0, 0.25 and 0.5. The gray dotted line is an example of finding combinations of $\hat{u}$ and η_c for a fixed value of $x^{(c)}$ and $x^{(h)}$. These combinations achieve maximum power. The figures (a) and (b) are basically Fig. 6.5 and 6.6, but the axes are swapped.